

# Thermal Fermion Propagators and Flavor-Changing via Loop Corrections in the Early Universe

---

A. Hataei<sup>1</sup> and S. S. Gousheh<sup>2</sup>

*Department of Physics, Shahid Beheshti University,  
Tehran, Iran*

ABSTRACT: We present the Minimally Extended Standard Model in the mass basis in the symmetric phase of the early Universe, demonstrating that the CP-violating CKM and PMNS matrices emerge not only in the weak interactions but also in the Yukawa interactions. This is due to the presence of all four components of the Higgs field and leads to a violation of fermion flavor conservation, a phenomenon absent in the broken phase. Specifically, left-handed fermions acquire additional thermal mass contributions involving the absolute values of CKM and PMNS matrix elements. Most notably, the structure of Yukawa interactions enables flavor-changing and CP-violating transitions among left-handed fermions, such as  $u_L \leftrightarrow c_L$ , which do not occur in the broken phase. In contrast, the right-handed fermions retain their mass eigenstates, leading to distinct thermal masses. Additionally, we identify novel CP-violating scattering processes, such as  $u_L \bar{c}_L \rightarrow 2A_3$ , which are exclusive to the symmetric phase.

---

<sup>1</sup>a.hataei@alumni.sbu.ac.ir

<sup>2</sup>ss-gousheh@sbu.ac.ir

---

## Contents

<b>1</b>	<b>Introduction</b>	<b>1</b>
<b>2</b>	<b>The Minimally Extended Standard Model in the Symmetric Phase</b>	<b>3</b>
<b>3</b>	<b>The Fermion Propagators and Their Thermal Masses</b>	<b>8</b>
<b>4</b>	<b>Flavor-Changing Processes of the Left-Handed Fermions</b>	<b>13</b>
<b>5</b>	<b>The Scattering Processes</b>	<b>17</b>
<b>6</b>	<b>Summary and Conclusion</b>	<b>17</b>
	<b>Appendices</b>	<b>18</b>
<b>A</b>	<b>Thermal Mass Calculations</b>	<b>18</b>
<b>B</b>	<b>Proof of the Absence of Flavor-Changing Processes for the Right-Handed Fermions</b>	<b>23</b>

---

## 1 Introduction

Quantum field theory at finite temperature (QFTFT) [1–4] is used to study a wide range of phenomena, including the early Universe [5–7], high-energy particle collisions [8], neutron stars [1], and phase transition [9, 10]. In general, there are two main approaches to quantum field theory at finite temperature: imaginary-time and real-time formalisms, both of which are reviewed in Ref [11]. In the imaginary-time formalism, using the analogy between inverse temperature  $T^{-1}$  and imaginary-time, Matsubara [12] developed a diagrammatic perturbation theory for the grand canonical partition function in the context of basic quantum field theory. This framework results in a temperature-dependent time-ordered propagator, commonly called the Matsubara propagator. On the other hand, the real-time formalism is essential for addressing dynamic questions [11]. This implies that the imaginary-time propagators must be extended to real-time propagators by analytic continuation, which yields either a retarded or advanced temperature-dependent propagator [2]. There are two approaches to the real-time formalism: one is the path integral method, also known as the closed-time path formalism [11], and the other is the operator method, referred to as thermofield dynamics [13]. In this paper, we use the imaginary time formalism since it suffices for our purposes.

In the electroweak phase transition (EWPT), the  $SU(2)_L \times U(1)_Y$  symmetry is spontaneously broken to  $U(1)_{EM}$  by the Higgs mechanism [14–16]. However, this symmetry

is restored in the symmetric phase, *i.e.*, for temperatures  $T > T_{\text{EWPT}} \approx 100\text{GeV}$  [17–21]. Indeed, the sign of the effective mass-squared in the Higgs potential caused by thermal corrections at the one-loop order changes at the  $T_{\text{EWPT}}$ , becoming positive in the symmetric phase [22]. One of the characteristics of the symmetric phase, which is crucial in this paper, is the restoration of all four degrees of freedom of the complex Higgs field  $\Phi = (\phi^+, \phi^0)$ .

The finite temperature propagators and their thermal masses play a prominent role in the calculation of many processes, particularly in the early universe, such as the effective Higgs potential and the Electroweak Phase transition within the SM model and beyond [23, 24], baryon asymmetry [25, 26], dilepton production rate [27], photon production rate [28], single quark and quark-antiquark potentials [29–31], fermion damping rate [32, 33], photon damping rate [34], gluon damping rate [35], the parton energy-loss [4], the transport coefficients of transient hydrodynamics [36], properties of dark matter [37, 38], gravitational wave signals [39], and thermodynamics quantities such as free energy, pressure, and number densities [4]. Furthermore, the thermal masses play a crucial role in hard-thermal-loop calculations (HTL), including HTL-improved Lagrangian [4, 40–43] and HTL perturbation theory (HTLpt) [44–48], where the latter is used to study the various physical quantities such as hydrodynamic properties [44–48].

In this study, we delve into the fermionic thermal masses and flavor-changing phenomena by formulating the MESM in the mass basis in the symmetric phase. As we shall demonstrate, the CP-violating Cabibbo-Kobayashi-Maskawa (CKM) [49, 50] and Pontecorvo [51]-Maki-Nakawaga-Sakata [52] (PMNS) matrices arise in the Yukawa interactions for  $\phi^{(+)}$  sector, in addition to their usual presence in the weak interactions. These findings stand in stark contrast to the broken phase, where such matrices only emerge in weak interactions. This phenomenon results in the manifestation of the absolute values of CKM and PMNS components in the thermal masses of left-handed quarks and leptons. Most notably, CP-violating matrices in Yukawa interactions enable flavor transitions among the left-handed fermions—an effect absent in the broken phase under the assumption of unitary PMNS and CKM matrices. For instance, at one-loop order, the left-handed up-quark  $u_L$  can propagate into the left-handed charm-quark  $c_L$ . Interestingly, its counterpart,  $c_L \rightarrow u_L$ , differs, indicating simultaneous CP and flavor violation at higher orders. While CP violation exists in the broken phase due to the CP-violating matrices, flavor violation is highly suppressed due to both the Glashow-Iliopoulos-Maiani (GIM) mechanism [53] and the Flavor-Changing Neutral Current (FCNC) theorem [54]. These constraints ensure that in the broken phase, flavor-changing processes only appear in the box diagrams. However, in the symmetric phase, the structure of the Yukawa interactions changes due to the presence of two complex Higgs bosons, allowing flavor-changing effects to arise at the one-loop order of self-energies and vertex diagrams. This mechanism naturally circumvents the suppression indicated by the GIM mechanism and FCNC theorem, making flavor violation for left-handed fermions an intrinsic feature of the symmetric phase. Additionally, we explore novel scattering processes such as  $u_L \bar{c}_L \rightarrow 2A_3$ , which are allowed in the symmetric phase. This process differs significantly from its counterpart,  $\bar{u}_L c_L \rightarrow 2A_3$ , providing a clear demonstration of CP violation. Furthermore, we show how our results reduce to those of the SM in the appropriate limit.

The paper is organized as follows. In Sec. (2) we express the MESM Lagrangian in the symmetric phase in the mass basis. In Sec. (3) we calculate the thermal masses, taking into account the contributions from all interactions. In Sec. (4) we demonstrate the flavor-changing processes for the left-handed fermions and discuss the resulting non-diagonal thermal mass-squared matrix. In Sec. (5) we explore some novel scattering processes. In Sec. (6), we present a summary and state our conclusions.

## 2 The Minimally Extended Standard Model in the Symmetric Phase

In the MESM, the asymmetry in the SM between the lepton and quark sectors due to the absence of right-handed neutrino fields is eliminated [55]. The study of electroweak interactions can be studied separately from strong interactions because there is no mixing between the  $SU(3)_C$  and  $SU(2)_L \times U(1)_Y$  sectors [55]. Without considering  $SU(3)_C$ , the MESM Lagrangian is written as follows:

$$\begin{aligned}
\mathcal{L} = & i \sum_{i=1,2,3} \bar{Q}_i \not{D} Q_i + i \sum_{i=1,2,3} \bar{L}_i \not{D} L_i + i \sum_{i=1,2,3} \bar{\nu}_{i_R} \not{\partial} \nu_{i_R} \\
& + i \sum_{i=1,2,3} \bar{e}_{i_R} \not{D} e_{i_R} + i \sum_{i=1,2,3} \bar{u}_{i_R} \not{D} u_{i_R} + i \sum_{i=1,2,3} \bar{d}_{i_R} \not{D} d_{i_R} \\
& - \frac{1}{4} B_{\mu\nu} B^{\mu\nu} - \frac{1}{4} A_{\mu\nu}^a A^{a\mu\nu} - \frac{1}{2\xi'} (\partial^\mu A_\mu^a)^2 + \bar{c}^a (-\partial^\mu D_\mu^{ab}) c^b \\
& + (D_\mu \Phi)^\dagger D^\mu \Phi - \mu^2 (T) \Phi^\dagger \Phi - \lambda (\Phi^\dagger \Phi)^2 \\
& - \sum_{i,j=1,2,3} \bar{L}_i \Lambda_{ij}^e \Phi e_{j_R} - \sum_{i,j=1,2,3} \bar{e}_{i_R} \Phi^\dagger \Lambda_{ij}^{e*} L_j \\
& - \sum_{i,j=1,2,3} \bar{L}_i \Lambda_{ij}^\nu \tilde{\Phi} \nu_{j_R} - \sum_{i,j=1,2,3} \bar{\nu}_{i_R} \tilde{\Phi}^\dagger \Lambda_{ij}^{\nu*} L_j \\
& - \sum_{i,j=1,2,3} \bar{Q}_i \Lambda_{ij}^d \Phi d_{j_R} - \sum_{i,j=1,2,3} \bar{d}_{i_R} \Phi^\dagger \Lambda_{ij}^{d*} Q_j \\
& - \sum_{i,j=1,2,3} \bar{Q}_i \Lambda_{ij}^u \tilde{\Phi} u_{j_R} - \sum_{i,j=1,2,3} \bar{u}_{i_R} \tilde{\Phi}^\dagger \Lambda_{ij}^{u*} Q_j.
\end{aligned} \tag{2.1}$$

Here  $D_\mu = \partial_\mu + igA_\mu^a \tau_a + ig' \frac{Y}{2} B_Y$  represents the covariant derivative, where  $\tau_a = \sigma_a/2$  ( $a = 1, 2, 3$ ) are the  $SU(2)_L$  generators with corresponding gauge boson fields  $A_\mu^a$ , and  $B_Y$  is the  $U(1)_Y$  gauge boson. The chiral components for the three generations of quarks and leptons are represented by the following doublets and singlets:

$$Q_i \equiv \begin{pmatrix} u_{i_L} \\ d_{i_L} \end{pmatrix}, \quad L_i \equiv \begin{pmatrix} \nu_{i_L} \\ e_{i_L} \end{pmatrix}, \quad u_{i_R}, \quad d_{i_R}, \quad \nu_{i_R}, \quad e_{i_R}, \quad i = 1, 2, 3, \tag{2.2}$$

where  $Q_i$ ,  $L_i$ ,  $u_{i_R}$ ,  $d_{i_R}$ ,  $\nu_{i_R}$ , and  $e_{i_R}$  represent the left-handed quark doublets, left-handed lepton doublets, right-handed up-quarks, right-handed down-quarks, right-handed neutrinos, and right-handed charged leptons, respectively, and  $i$  denotes the generation's index.

The Higgs doublet is defined as follows:

$$\Phi = \begin{pmatrix} \phi^{(+)} \\ \phi^{(0)} \end{pmatrix}, \quad (2.3)$$

where  $\phi^{(+)}$  and  $\phi^{(0)}$  represent charged and neutral complex scalar fields, and the doublet  $\tilde{\Phi} := i\sigma_2\Phi^*$ . The first and second lines include the kinetic terms of fermions and their interactions with gauge fields. The third line includes the kinetic terms of the gauge fields  $B_\mu$  and  $A_\mu^a$ , along with their gauge fixing terms, the latter being the Faddeev-Popov ghost term. The fourth line contains the free and self-interacting parts of the Higgs doublets, which includes the effective-mass-squared term  $\mu^2(T)$ , which is positive in the symmetric phase [22]. The  $\mu^2(T)$  derived from the one-loop effective Higgs potential [22] is relevant here, though its explicit form is not required for this study. The fifth, sixth, seventh, and eighth lines encompass the Yukawa interactions, where  $A_{ij}^\nu$ ,  $A_{ij}^e$ ,  $A_{ij}^d$ , and  $A_{ij}^u$  are the Yukawa coupling constants for neutrinos, charged leptons, down-quarks, and up-quarks, respectively. These coupling constants are not generally diagonal, although they can be diagonalized in the mass basis, which will be discussed in the following. Note that the only difference between the SM and MESM is the presence of right-handed neutrinos along with nonzero Yukawa coupling constants  $A_{ij}^\nu$ , with which the neutrinos acquire Dirac masses in the broken phase via the Higgs mechanism. It is worth mentioning that the coupling constant  $\lambda$  also has thermal corrections [56, 57], which have a negligible effect on our study.

The mass basis is defined as the one in which the Yukawa matrices  $A_{ij}^\nu$ ,  $A_{ij}^e$ ,  $A_{ij}^d$ , and  $A_{ij}^u$  are all diagonal. This can be achieved, for example, by starting with the weak interaction basis and using appropriate chiral transformations on the fermion fields. The chiral transformations between the left-handed (right-handed) quarks in flavor basis ( $q_i$ ) and the mass basis ( $q'_j$ ) are achieved by the unitary matrices  $U_Q^{ij}$  ( $W_u^{ij}$  and  $W_d^{ij}$ ), as follows,

$$Q_i \rightarrow U_Q^{ij} Q'_j = \begin{pmatrix} U_u^{ij} & 0 \\ 0 & U_d^{ij} \end{pmatrix} \begin{pmatrix} u'_{jL} \\ d'_{jL} \end{pmatrix}, \quad u_{iR} \rightarrow W_u^{ij} u'_{jR}, \quad d_{iR} \rightarrow W_d^{ij} d'_{jR}, \quad i, j = 1, 2, 3, \quad (2.4)$$

with the unitarity condition  $U_u U_u^\dagger = U_d U_d^\dagger = W_u W_u^\dagger = W_d W_d^\dagger = \mathbb{1}$ . These matrices are chosen such that the Yukawa coupling constants  $A_{ij}^d$  and  $A_{ij}^u$  become diagonal as follows:

$$\begin{aligned} \lambda^d &= U_d^\dagger A^d W_d = \begin{pmatrix} \lambda_{11}^d & 0 & 0 \\ 0 & \lambda_{22}^d & 0 \\ 0 & 0 & \lambda_{33}^d \end{pmatrix} \equiv \begin{pmatrix} \lambda^{d_1} & 0 & 0 \\ 0 & \lambda^{d_2} & 0 \\ 0 & 0 & \lambda^{d_3} \end{pmatrix} \equiv \begin{pmatrix} \lambda^d & 0 & 0 \\ 0 & \lambda^s & 0 \\ 0 & 0 & \lambda^b \end{pmatrix}, \\ \lambda^u &= U_u^\dagger A^u W_u = \begin{pmatrix} \lambda_{11}^u & 0 & 0 \\ 0 & \lambda_{22}^u & 0 \\ 0 & 0 & \lambda_{33}^u \end{pmatrix} \equiv \begin{pmatrix} \lambda^{u_1} & 0 & 0 \\ 0 & \lambda^{u_2} & 0 \\ 0 & 0 & \lambda^{u_3} \end{pmatrix} \equiv \begin{pmatrix} \lambda^u & 0 & 0 \\ 0 & \lambda^c & 0 \\ 0 & 0 & \lambda^t \end{pmatrix}. \end{aligned} \quad (2.5)$$

Here  $\lambda_{ij}^d$  and  $\lambda_{ij}^u$  are the diagonal coupling constants for down-quarks and up-quarks, respectively. Using these transformations in Eq. (2.4), the Lagrangian corresponding to the

quarks part in Eq. (2.1) becomes

$$\begin{aligned}
\mathcal{L}'_{Quarks} = & i\bar{Q}'_m (U_Q^{mi*} \not{D} U_Q^{in}) Q'_n + i\bar{u}'_{mR} (W_u^{mi*} \not{D} W_u^{in}) u'_{nR} + i\bar{d}'_{mR} (W_d^{mi*} \not{D} W_d^{in}) d'_{nR} \\
& - \bar{Q}'_m \left( U_Q^{mi*} \Lambda_{ij}^d \not{D} W_d^{jn} \right) d'_{nR} - \bar{d}'_{mR} \left( W_d^{mi*} \Phi^\dagger \Lambda_{ij}^{d*} U_Q^{jn} \right) Q'_n \\
& - \bar{Q}'_m \left( U_Q^{mi*} \Lambda_{ij}^u \tilde{\not{D}} W_u^{jn} \right) u'_{nR} - \bar{u}'_{mR} \left( W_u^{mi*} \tilde{\Phi}^\dagger \Lambda_{ij}^{u*} U_Q^{jn} \right) Q'_n.
\end{aligned} \tag{2.6}$$

In the first line, considering that the unitarity of chiral transformation and their commutation with the generators of symmetry group  $SU(2)_L \times U(1)_Y$ , the matrices  $W_u$  and  $W_d$  in the second and third terms cancel out, while for the first term, the CKM matrix emerges, similarly to the broken phase:

$$i\bar{Q}'_m (U_Q^{mi*} \not{D} U_Q^{in}) Q'_n = i\bar{Q}'_m \begin{pmatrix} \delta_{mn} (\not{D} + \frac{ig}{2} \mathcal{A}_3 + \frac{i}{2} g' \mathcal{B}_Y Y) & V_{mn} \left( \frac{ig}{2} (\mathcal{A}_1 - i\mathcal{A}_2) \right) \\ V_{mn}^* \left( \frac{ig}{2} (\mathcal{A}_1 + i\mathcal{A}_2) \right) & \delta_{mn} (\not{D} - \frac{ig}{2} \mathcal{A}_3 + \frac{i}{2} g' \mathcal{B}_Y Y) \end{pmatrix} Q'_n, \tag{2.7}$$

where  $V$  is the CKM matrix  $V = U_u^\dagger U_d$ , the final form of which includes three angles and one phase, the latter being a source of CP violation [55, 58]. For the first term in the second line of Eq. (2.6), we have

$$\begin{aligned}
U_Q^{mi*} \Lambda_{ij}^d \not{D} W_d^{jn} &= \begin{pmatrix} U_u^{mi*} \Lambda_{ij}^d \phi^{(+)} W_d^{jn} \\ U_d^{mi*} \Lambda_{ij}^d \phi^{(0)} W_d^{jn} \end{pmatrix} = \begin{pmatrix} U_u^{ml*} U_d^{lk} U^{ki*} \Lambda_{ij}^d W_d^{jn} \phi^{(+)} \\ U_d^{mi*} \Lambda_{ij}^d W_d^{jn} \phi^{(0)} \end{pmatrix} \\
&= \begin{pmatrix} V_{mk} \lambda_{kn}^d \phi^{(+)} \\ \lambda_{mn}^d \phi^{(0)} \end{pmatrix} = \begin{pmatrix} V_{mk} & 0 \\ 0 & \delta_{mk} \end{pmatrix} \lambda_{kn}^d \begin{pmatrix} \phi^{(+)} \\ \phi^{(0)} \end{pmatrix} \equiv \mathcal{V}'_{mk} \lambda_{kn}^d \tilde{\Phi},
\end{aligned} \tag{2.8}$$

and the second term in the second line of Eq. (2.6) is the hermitian conjugate of the above equation. For the first term in the third line of Eq. (2.6), we have

$$\begin{aligned}
U_Q^{mi*} \Lambda_{ij}^u \tilde{\not{D}} W_u^{jn} &= \begin{pmatrix} U_u^{mi*} \Lambda_{ij}^u \phi^{(0)*} W_u^{jn} \\ -U_d^{mi*} \Lambda_{ij}^u \phi^{(+)*} W_u^{jn} \end{pmatrix} = \begin{pmatrix} U_u^{mi*} \Lambda_{ij}^u W_u^{jn} \phi^{(0)*} \\ -U_d^{ml*} U^{lk} U^{ki*} \Lambda_{ij}^u W_u^{jn} \phi^{(+)*} \end{pmatrix} \\
&= \begin{pmatrix} \lambda_{mn}^u \phi^{(0)*} \\ -V_{mk}^* \lambda_{kn}^u \phi^{(+)*} \end{pmatrix} = \begin{pmatrix} \delta_{mk} & 0 \\ 0 & V_{mk}^* \end{pmatrix} \lambda_{kn}^u \begin{pmatrix} \phi^{(0)*} \\ -\phi^{(+)*} \end{pmatrix} \equiv \mathcal{V}''_{mk} \lambda_{kn}^u \tilde{\Phi},
\end{aligned} \tag{2.9}$$

and the second term in the third line of Eq. (2.6) is the hermitian conjugate of the above equation. Consequently, the Lagrangian corresponding to the quark parts in the symmetric

phase is outlined below

$$\begin{aligned}
\mathcal{L}'_{Quarks} = & i \sum_{i,j=1,2,3} \bar{Q}'_m (U_Q^{mi*} \not{D} U_Q^{in}) Q'_n + i \sum_{i=1,2,3} \bar{u}'_{iR} \not{D} u'_{iR} + i \sum_{i=1,2,3} \bar{d}'_{iR} \not{D} d'_{iR} \\
& - \sum_{i,j,n=1,2,3} \bar{Q}'_i \mathcal{V}'_{ij} \lambda_{jn}^d \not{\Phi} d'_{nR} - \sum_{i,j,n=1,2,3} \bar{d}'_{iR} \not{\Phi}^\dagger \lambda_{ij}^{d*} \mathcal{V}'_{jn}{}^* Q'_n \\
& - \sum_{i,j,n=1,2,3} \bar{Q}'_i \mathcal{V}''_{ij} \lambda_{jn}^u \not{\tilde{\Phi}} u'_{nR} - \sum_{i,j,n=1,2,3} \bar{u}'_{iR} \not{\tilde{\Phi}}^\dagger \lambda_{ij}^{u*} \mathcal{V}''_{jn}{}^* Q'_n.
\end{aligned} \tag{2.10}$$

Equation (2.10) shows that in the symmetric phase, the CKM matrix is present not only in the weak interactions but also in the Yukawa interactions. This stands in contrast to the broken phase, where it exclusively appears in weak interactions. The appearance of the CKM matrix in the Yukawa interactions is due to the existence of  $\phi^{(+)}$ . To clarify this issue, consider the first term in the second line of Eq. (2.10), the explicit form of which is,

$$-\bar{u}'_{iL} V_{im} \lambda_{mj}^d \phi^{(+)} d'_{jR} - \bar{d}'_{iL} \lambda_{ij}^d \phi^{(0)} d'_{jR}. \tag{2.11}$$

This shows explicitly that the presence of the field  $\phi^{(+)}$  in the first term of Eq. (2.10), which contains a CP-violating term, leads to the mixing of different generations of quarks in the interactions in which  $\phi^{(+)}$  is the virtual particle. Hence, flavor-changing processes emerge at the one-loop level in left-handed fermion propagators—a phenomenon uniquely restricted to the symmetric phase. In Sec. (4), we will delve into this challenge. As we know, in the broken phase, only the second term survives, indicating that the tree-level masses and Higgs couplings are diagonal in flavor and preserve the discrete symmetries P, T, C [59]. The rest of the terms in the second and third lines of Eq. (2.10) can be similarly expressed.

The transformation between the mass and flavor bases for left-handed and right-handed neutrinos (charged leptons) is encoded in the unitary matrices  $U_L^{ij}$  and  $W_\nu^{ij}$  ( $W_e^{ij}$ ), given by the following chiral transformations

$$L_i \rightarrow U_L^{ij} L'_j = \begin{pmatrix} U_\nu^{ij} & 0 \\ 0 & U_e^{ij} \end{pmatrix} \begin{pmatrix} \nu'_{jL} \\ e'_{jL} \end{pmatrix}, \quad \nu_{iR} \rightarrow W_\nu^{ij} \nu'_{jR}, \quad e_{iR} \rightarrow W_e^{ij} e'_{jR}, \quad i, j = 1, 2, 3, \tag{2.12}$$

where  $U_\nu^\dagger U_\nu = U_e^\dagger U_e = W_l^\dagger W_l = \mathbb{1}$ . The calculations proceed analogously to those in the quark sector. The chiral transformation matrices are chosen so that the Yukawa coupling

constants of leptons become diagonal:

$$\begin{aligned}\lambda^\nu &= U_\nu^\dagger A^\nu W_\nu = \begin{pmatrix} \lambda_{11}^\nu & 0 & 0 \\ 0 & \lambda_{22}^\nu & 0 \\ 0 & 0 & \lambda_{33}^\nu \end{pmatrix} \equiv \begin{pmatrix} \lambda^{\nu_1} & 0 & 0 \\ 0 & \lambda^{\nu_2} & 0 \\ 0 & 0 & \lambda^{\nu_3} \end{pmatrix} \equiv \begin{pmatrix} \lambda^{\nu_e} & 0 & 0 \\ 0 & \lambda^{\nu_\mu} & 0 \\ 0 & 0 & \lambda^{\nu_\tau} \end{pmatrix}, \\ \lambda^e &= U_e^\dagger A^e W_e = \begin{pmatrix} \lambda_{11}^e & 0 & 0 \\ 0 & \lambda_{22}^e & 0 \\ 0 & 0 & \lambda_{33}^e \end{pmatrix} \equiv \begin{pmatrix} \lambda^{e_1} & 0 & 0 \\ 0 & \lambda^{e_2} & 0 \\ 0 & 0 & \lambda^{e_3} \end{pmatrix} \equiv \begin{pmatrix} \lambda^e & 0 & 0 \\ 0 & \lambda^\mu & 0 \\ 0 & 0 & \lambda^\tau \end{pmatrix}.\end{aligned}\tag{2.13}$$

where  $\lambda_{ij}^\nu$  and  $\lambda_{ij}^e$  are diagonal coupling constants for neutrinos and charged leptons, respectively. Similarly to the chiral transformation calculations for quarks, the Lagrangian corresponding to the lepton part in the mass basis can be written as (The expanded form is given in Eq. (B.1))

$$\begin{aligned}\mathcal{L}'_{Leptons} &= i \sum_{i,j=1,2,3} \bar{L}'_i \left( U_L^{im*} \not{D} U_L^{mj} \right) L'_j + i \sum_{i=1,2,3} \bar{e}'_{iR} \not{D} e'_{iR} + i \sum_{i=1,2,3} \bar{\nu}'_{iR} \not{D} \nu'_{iR} \\ &\quad - \sum_{i,j,n=1,2,3} \bar{L}'_i \mathcal{U}'_{ij} \lambda_{jn}^e \not{\Phi} e'_{nR} - \sum_{i,j,n=1,2,3} \bar{e}'_{iR} \not{\Phi}^\dagger \lambda_{ij}^{e*} \mathcal{U}'_{jn*} L'_n \\ &\quad - \sum_{i,j,n=1,2,3} \bar{L}'_i \mathcal{U}''_{ij} \lambda_{jn}^\nu \not{\tilde{\Phi}} \nu'_{nR} - \sum_{i,j,n=1,2,3} \bar{\nu}'_{iR} \not{\tilde{\Phi}}^\dagger \lambda_{ij}^{\nu*} \mathcal{U}''_{jn*} L'_n,\end{aligned}\tag{2.14}$$

where  $\mathcal{U}'_{ij}$  and  $\mathcal{U}''_{ij}$  are

$$\mathcal{U}'_{ij} = \begin{pmatrix} U_{ij} & 0 \\ 0 & \delta_{ij} \end{pmatrix}, \quad \mathcal{U}''_{ij} = \begin{pmatrix} \delta_{ij} & 0 \\ 0 & U_{ij}^* \end{pmatrix},\tag{2.15}$$

in which  $U = U_\nu^\dagger U_e$ , and is the PMNS matrix. Similar to the CP-violating CKM matrix, the CP-violating PMNS matrix has the same properties and appears in the Yukawa interactions, in addition to the weak interactions. The first term of the above equation is similar to Eq. (2.7) with the replacements of quark fields and the CKM matrix with the lepton fields and PMNS matrix, respectively. Note that, with the elimination of  $\nu_{nR}$ , Eq. (2.14) reduces to the leptonic part of the SM Lagrangian in the symmetric phase

$$\mathcal{L}'_{L,SM} = i \sum_{i=1,2,3} \bar{L}'_i \not{D} L'_i + i \sum_{i=1,2,3} i \bar{e}'_{iR} \not{D} e'_{iR} - \sum_{i,j=1,2,3} \bar{L}'_i \lambda_{ij}^l \not{\Phi} e'_{jR} - \sum_{i,j=1,2,3} \bar{e}'_{iR} \not{\Phi}^\dagger \lambda_{ij}^{l*} L'_j,\tag{2.16}$$

where  $\lambda^l$  is the Yukawa coupling constant matrix for charged leptons. As can be seen, the Yukawa coupling constants for the leptons become completely diagonal, and the PMNS matrix does not appear in either weak interactions or Yukawa interactions. This is due to the choice of chiral transformations for leptons  $U_\nu = U_e$ .





**Figure 1:** The self-energy diagrams for fermions at one-loop order with gauge and Yukawa interactions, respectively.

### 3 The Fermion Propagators and Their Thermal Masses

In this section, we discuss the fermion propagators and their thermal masses in the symmetric phase. The propagator for the massless fermions is written as [2]

$$S(P) = \frac{i}{\not{P} - \Sigma}, \quad (3.1)$$

where  $\Sigma$  is the self-energy of the fermion propagator at finite temperature, and  $P^\mu = (p_0, \vec{p})$  is the external four-momentum in Minkowski space-time. The one-loop order self-energy of the fermions consists of two separate parts corresponding to zero and finite temperature [60]

$$\Sigma^{(1)} \equiv \Sigma_{T=0}^{(1)} + \Sigma_T^{(1)}. \quad (3.2)$$

Let us now consider the self-energy diagrams at the one-loop order for gauge and Yukawa interactions depicted in Fig. 1. For both interactions, the finite temperature parts cannot be calculated exactly. However, they can be calculated in both high [2, 60] and low-temperature [61] limits. Thus, when calculating the fermion self-energy  $\Sigma_T$  in the symmetric phase, it is crucial to determine the appropriate temperature limit. The most significant contribution of temperature to the self-energy at the one-loop order is in the high-temperature limit, where the leading contribution is proportional to  $T^2$  [2, 60, 62]. In our case, the high-temperature regime is defined as the limit where the temperature  $T$  is much larger than the effective Higgs mass  $\mu(T)$  and external four-momentum ( $T \gg \mu(T), p^0, |\vec{p}|$ ) (see Fig. (1)). As mentioned before, the effective-mass-squared  $\mu^2(T)$ <sup>1</sup> is modified by the effects of QFTFT, and becomes positive  $\mu^2(T) > 0$  for  $T > T_{EW}$  [22]. In the high-temperature limit, calculations are typically performed using the HTL approximation. In this approximation, within the imaginary time formalism, the magnitudes of internal momenta are considered to be proportional to the temperature, i.e.,  $|\vec{k}|, k_0 \sim T$ , which are referred to as the hard momentum. Hence, this approximation amounts to  $|\vec{k}| \gg \{|\vec{p}|, \mu(T)\}$ <sup>2</sup> [2]. Using the HTL approximation for gauge and Yukawa interactions, the self-energy  $\Sigma_T$

<sup>1</sup>Note that the Higgs field has four degrees of freedom in the symmetric phase, with the same effective thermal mass, three of which are absorbed by the  $SU(2)_L$  gauge fields in the broken phase by the Higgs mechanism [59].

<sup>2</sup>In the real-time formalism the requirement  $\mu(T), P \ll K$  is sufficient [63]. The reason why we can neglect  $\mu(T)$  is discussed in detail in the Appendix (A).

is obtained as [2, 60]<sup>3</sup> (See Append. (A).)

$$\Sigma_T = \frac{m_f^2(T)}{|\vec{p}|} \gamma_0 \mathcal{Q}_0\left(\frac{p_0}{|\vec{p}|}\right) + \frac{m_f^2(T)}{|\vec{p}|} \vec{\gamma} \cdot \hat{p} \left[ 1 - \frac{p_0}{|\vec{p}|} \mathcal{Q}_0\left(\frac{p_0}{|\vec{p}|}\right) \right], \quad (3.3)$$

where  $p_0$  and  $|\vec{p}|$  are energy and magnitude of the external three-momentum, respectively. Moreover, For the retarded self-energy, the Legendre function  $\mathcal{Q}_0\left(\frac{p_0}{|\vec{p}|}\right)$  has the following form<sup>4</sup>:

$$\mathcal{Q}_0\left(\frac{p_0}{|\vec{p}|}\right) = \frac{1}{2} \ln \left| \frac{p_0 + |\vec{p}|}{p_0 - |\vec{p}|} \right| - \frac{i\pi}{2} \theta(|\vec{p}|^2 - p_0^2). \quad (3.4)$$

Furthermore,  $m_f(T)$  is the thermal mass, which is directly proportional to  $T$  and contains the coupling constants of the interactions. The contributions of the non-Abelian SU(N), Abelian U(1)<sub>Y</sub>, and Yukawa interactions to the thermal masses are given, in order, by [2, 60]

$$m_f^2(T) = g^2 \frac{T^2}{8} C_2(N) + \left( \frac{g'Y}{2} \right)^2 \frac{T^2}{8} + |\lambda|^2 \frac{T^2}{16}, \quad (3.5)$$

where  $g$ ,  $g'$ , and  $\lambda$  are coupling constants and  $C_2(N)$  is quadratic Casimir operator of the fermions, given by [59]

$$C_2(N) = \frac{N^2 - 1}{2N}. \quad (3.6)$$

That is, the form of the contributions to the self-energy for fermions coming from different interactions is the same as given by Eq. (3.3); The key distinction lies in the thermal masses, which alter the dispersion relations of propagators [2, 60]. The self-energy  $\Sigma_{T=0}$  for massless fermions have both UV and IR divergences. The UV divergence can be removed through renormalization at finite temperature, and the Kinoshita-Lee-Nauenberg (KLN) theorem [66, 67] ensures that IR divergences cancel out when physical observables are considered. It is worth noting that, for the finite temperature contribution  $\Sigma_T$ , UV divergences do not arise because the distribution functions fall off exponentially at high energies. Additionally, IR divergences do not emerge at the one-loop order when the high-temperature limit is employed. On the other hand, in the low-temperature limit, the IR divergences that arise at the one-loop order cancel out exactly when physical quantities are considered [68]. Furthermore, in general, the renormalization at finite temperature differs from common renormalization at zero temperature [68–71]. However, after renormalization, the finite terms in the self-energy  $\Sigma_{T=0}$  can be safely ignored, as they are negligible compared to the  $T^2$ -terms in the high-temperature limit [2]. Hence, in the following, we calculate  $\Sigma_T$  using the high-temperature limit and neglect  $\Sigma_{T=0}$ . Furthermore, since the left- and right-handed

<sup>3</sup>The rest of the contributions are proportional to  $T$  and  $\log(T)$  [64, 65] which are negligible, as compared to  $T^2$ , in the high temperature limit.

<sup>4</sup>This Legendre function is written for the retarded self-energy, which in the complex energy plane we have  $q_0 + i\eta$ , where  $\eta \rightarrow 0$ . One may write the advanced self-energy, which in the complex energy plane we have  $q_0 - i\eta$ , and the form of the Legendre function is [2]

$$\mathcal{Q}_0\left(\frac{p_0}{|\vec{p}|}\right) = \frac{1}{2} \ln \left| \frac{p_0 + |\vec{p}|}{p_0 - |\vec{p}|} \right| + \frac{i\pi}{2} \theta(|\vec{p}|^2 - p_0^2).$$

fermions experience different interactions, we calculate their thermal masses separately.

At this stage, we aim to calculate the fermionic thermal masses in the symmetric phase of the early Universe within the MESM in the mass basis, and subsequently reduce the results to the Standard Model (SM). To accomplish this, we employ the MESM Lagrangian formulated in Section (2), which includes weak, hypercharge, and Yukawa interactions. For quarks, the covariant derivative also incorporates SU(3) gauge interactions, leading to an additional contribution to the thermal mass of quarks, which will be taken into account. To calculate the contributions of quark thermal masses, we first expand Eq. (2.10) as follows

$$\begin{aligned}
\mathcal{L}'_{Quarks} = & i\bar{u}'_{i_L} \left( \not{\partial} + \frac{ig}{2} \mathcal{A}_3 + \frac{i}{6} g' \not{B}_Y \right) u'_{i_L} + i\bar{u}'_{i_L} \left( V_{ij} \frac{ig}{2} (\mathcal{A}_1 - i\mathcal{A}_2) \right) d'_{j_L} \\
& + i\bar{d}'_{i_L} \left( V_{ij}^* \left( \frac{ig}{2} (\mathcal{A}_1 + i\mathcal{A}_2) \right) \right) u'_{j_L} + i\bar{d}'_{i_L} \left( \not{\partial} - \frac{ig}{2} \mathcal{A}_3 + \frac{i}{6} g' \not{B}_Y \right) d'_{i_L} \\
& + i\bar{u}'_{i_R} \left( \not{\partial} + i\frac{2}{3} g' \not{B}_Y \right) u'_{i_R} + i\bar{d}'_{i_R} \left( \not{\partial} - i\frac{2}{6} g' \not{B}_Y \right) d'_{i_R} \\
& - \left\{ \bar{u}'_{i_L} V_{im} \lambda_{mj}^d \phi^{(+)} d'_{j_R} + \bar{d}'_{i_L} \lambda_{ij}^d \phi^{(0)} d'_{j_R} \right\} - H.C. \\
& - \left\{ \bar{u}'_{i_L} \lambda_{ij}^u \phi^{(0)*} u'_{j_R} - \bar{d}'_{i_L} V_{im}^* \lambda_{mj}^u \phi^{(+)*} u'_{j_R} \right\} - H.C,
\end{aligned} \tag{3.7}$$

where ‘ $H.C$ ’ denotes the Hermitian conjugate of the terms in the curly brackets. Here, we define  $A^\pm = \frac{1}{\sqrt{2}}(\mathcal{A}_1 \mp i\mathcal{A}_2)$ . Now, we focus on cases where identical particles appear in both the initial and final states: No flavor-changing occurs. To clarify, the self-energy corrections for  $u_{i_L}$  and  $u_{i_R}$  are shown in Figs. (2) and (3), where ‘ $i$ ’ denotes the generation’s index, and the Einstein summation is used for the remaining indices. Using Eq. (3.5), the diagonality of the Yukawa coupling constants, and the unitarity of the CKM matrix, we calculate the quark thermal masses, as detailed in Append. (A) for  $u_{i_L}$  and  $u_{i_R}$ . The remaining cases are acquired similarly, and the final results are outlined as follows<sup>5</sup>:

$$\begin{aligned}
m_{u_{i_R}}^2(T) &= \frac{g^2 T^2}{18} + \frac{g'^2 T^2}{6} + \frac{|\lambda^{u_i}|^2 T^2}{8}, \\
m_{d_{i_R}}^2(T) &= \frac{g^2 T^2}{72} + \frac{g'^2 T^2}{6} + \frac{|\lambda^{d_i}|^2 T^2}{8}, \\
m_{u_{i_L}}^2(T) &= \frac{g^2 T^2}{288} + \frac{3g^2 T^2}{32} + \frac{g'^2 T^2}{6} + (|\lambda^{u_i}|^2 + |V_{ij} \lambda^{d_j}|^2) \frac{T^2}{16}, \\
m_{d_{i_L}}^2(T) &= \frac{g^2 T^2}{288} + \frac{3g^2 T^2}{32} + \frac{g'^2 T^2}{6} + (|\lambda^{d_i}|^2 + |V_{ij}^* \lambda^{u_j}|^2) \frac{T^2}{16}.
\end{aligned} \tag{3.8}$$

Since the right-handed quarks are singlet under the SU(2)<sub>L</sub> interaction, they do not receive contributions from this interaction. For the weak interactions, although the CKM matrix appears in the Lagrangian, it does not contribute to the fermion thermal masses due to the CKM unitarity. The same applies to Yukawa couplings for right-handed quarks—their

<sup>5</sup>We exclusively use perturbation theory to compute thermal masses, including those arising from the Yukawa coupling of the top quark ( $\lambda^t$ ), following Refs. [22, 23, 72]. In principle, the effects of  $\lambda^t$  should be studied using non-perturbative methods, not only for the right- and left-handed top quark thermal masses but also for the Higgs potential. However, we postpone it to future studies.

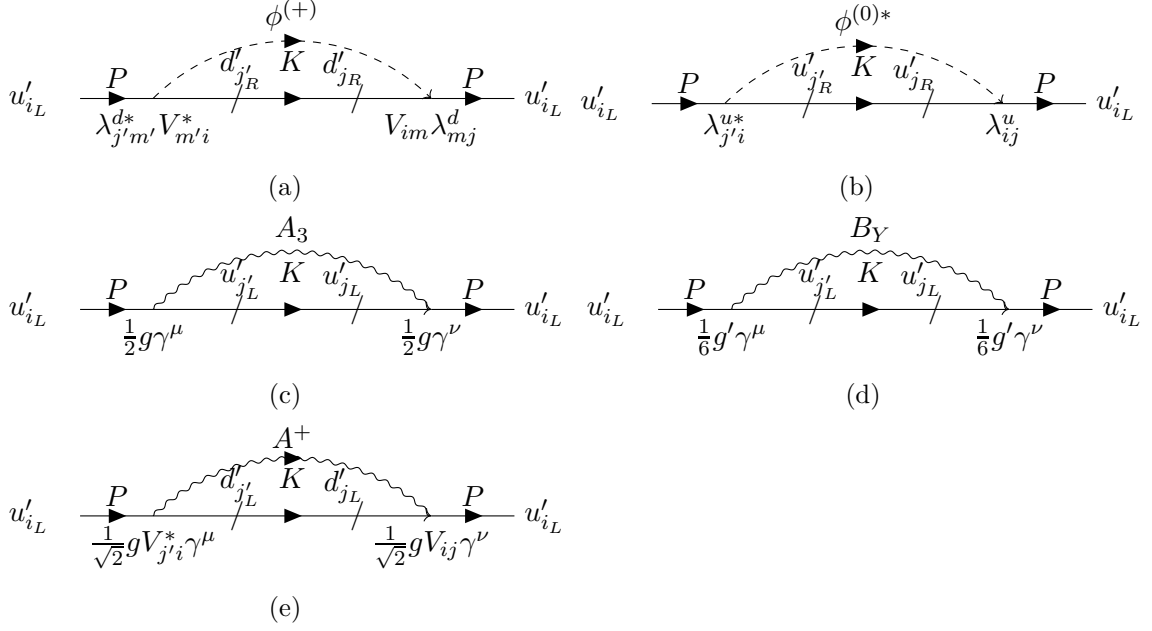


**Figure 2:** The Feynman diagrams (in imaginary-time formalism) that contribute to the left-handed up-quarks encompass electro-weak interactions in the symmetric phase. Here,  $K$  indicates the momentum of scalars or gauge bosons, and the momentum of internal fermions is  $P - K$ .

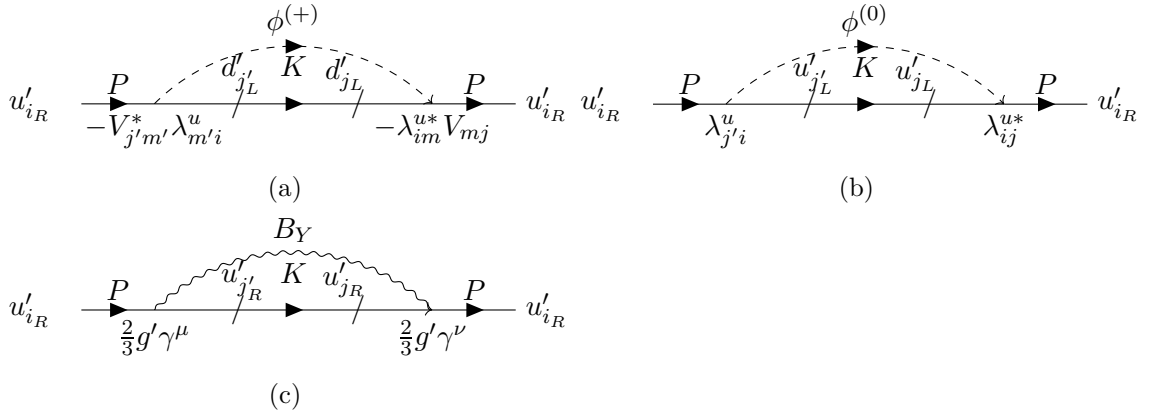


**Figure 3:** The Feynman diagrams (in imaginary-time formalism) of the right-handed up-quarks.

thermal masses remain unaffected by CKM components. In contrast, for the left-handed quarks, the absolute values of the CKM matrix contribute to the thermal masses- the consequence of considering the mass basis and the emerging CKM matrix in the Lagrangian. Notably, the off-diagonal components of the CKM matrix do not vanish due to the coupling constants  $\lambda^d$ ,  $\lambda^s$ , and  $\lambda^b$  are different. To clarify this issue, consider the thermal mass of the left-handed up-quarks

$$\begin{aligned} m_{u_{iL}}^2(T) &= \frac{g'^2 T^2}{288} + \frac{3g^2 T^2}{32} + \frac{g''^2 T^2}{6} + (|\lambda^{u_i}|^2 + |\lambda^{d_j} V_{ji}|^2) \frac{T^2}{16}, \\ &= \frac{g'^2 T^2}{288} + \frac{3g^2 T^2}{32} + \frac{g''^2 T^2}{6} + \left( |\lambda^{u_i}|^2 + |\lambda^d V_{1i}|^2 + |\lambda^s V_{2i}|^2 + |\lambda^b V_{3i}|^2 \right) \frac{T^2}{16}, \end{aligned} \quad (3.9)$$

where the explicit mixing of  $\lambda^{d_j} V_{ji}$  is determined. As a result, the contributions of  $\lambda^d$  to the thermal masses of left-handed quarks involve a mixing of CKM components. If only  $|\lambda^{d_i}|^2$  appeared in the thermal masses, it would indicate that no mixing occurs between different generations. However, for instance, in the case of the first-generation up-quark, the thermal mass contributions involve a combination of  $\lambda^d$ ,  $\lambda^s$ , and  $\lambda^b$ . This suggests that the Yukawa sector may play a crucial role in enabling flavor-changing between the different generations. Conversely, the right-handed quarks have distinct thermal masses, which ensures us no mixing in flavors occurs.

Now, for the lepton sector, using Eq. (3.5) (with its expanded form provided in Eq. (B.1)) and following the same approach as for quarks, we calculate the lepton thermal masses, which are outlined below

$$\begin{aligned} m_{\nu_{iR}}^2(T) &= \frac{|\lambda^{\nu_i}|^2 T^2}{8}, \\ m_{e_{iR}}^2(T) &= \frac{g'^2 T^2}{8} + \frac{|\lambda^{e_i}|^2 T^2}{8}, \\ m_{\nu_{iL}}^2(T) &= \frac{g'^2 T^2}{32} + \frac{3g^2 T^2}{32} + (|\lambda^{\nu_i}|^2 + |U_{ij} \lambda^{e_j}|^2) \frac{T^2}{16}, \\ m_{e_{iL}}^2(T) &= \frac{g'^2 T^2}{32} + \frac{3g^2 T^2}{32} + (|\lambda^{e_i}|^2 + |U_{ij}^* \lambda^{\nu_j}|^2) \frac{T^2}{16}. \end{aligned} \quad (3.10)$$

The results of thermal masses can be reduced to the SM (in the mass basis), and the only differences are related to the lepton parts. We have used Eq. (2.16), in which the thermal masses of the leptons are outlined as follows

$$\begin{aligned} m_{iL}^2(T) &= \frac{g'^2 T^2}{32} + \frac{3g^2 T^2}{32} + \frac{|\lambda^{l_i}|^2 T^2}{16}, \\ m_{e_{iR}}^2(T) &= \frac{g'^2 T^2}{8} + \frac{|\lambda^{l_i}|^2 T^2}{8}. \end{aligned} \quad (3.11)$$

Here, the index ‘ $L$ ’ refers to both the left-handed neutrinos and charged leptons. In this case, the thermal mass of the right-handed leptons arising from Yukawa interactions is twice that of the left-handed leptons due to their Higgs channel interactions. Because the

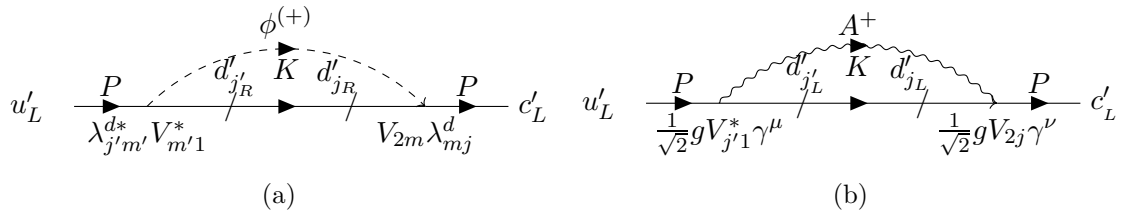


**Figure 4:** The Feynman diagrams (in imaginary-time formalism) demonstrate the propagation of the left-handed up-quark to the charm quark. Here,  $K$  indicates the momentum of scalars or gauge bosons, and the momentum of internal fermions is  $P - K$ .

corresponding Lagrangian to leptons is fully diagonal, flavor mixing does not occur in the self-energies. It is worth noting that lepton thermal masses in the SM have been studied in Ref. [25], where the authors also computed quark thermal masses. However, they neglected CKM effects, assuming they were negligible. As this assumption is incomplete, we demonstrate the crucial effect of the CP-violating matrices in Sec. (4).

The HTL approximation is invalid for calculating self-energies (or thermal masses) in the broken phase, as tree-level (physical) masses are extremely large at temperatures below  $\sim 100$  GeV: The three-level masses of weak gauge bosons, Higgs boson, and top quark, respectively, are  $\sim 80, 125, 170$  GeV. Hence, according to Eq. (A.10), it is impossible to neglect the three-level masses in comparison to the internal momenta, making the consideration of the HTL approximation incorrect.

#### 4 Flavor-Changing Processes of the Left-Handed Fermions

In this section, we aim to demonstrate the flavor transformation for the left-handed fermions. The sectors that contain CP-violating matrices, due to their mixing properties, can only enable flavor-changing phenomena at the one-loop order. For clarity, we first examine the propagation of  $u_L$  to  $c_L$ , as shown in Fig. 4. Following the approach outlined in Append. (A), the self-energy for diagram (b), employing the HTL approximation, is given by

$$\Sigma_{u_L-c_L}^{(b)}(P) \approx -\frac{1}{4}g^2V_{j'1}^*V_{2j}\delta_{jj'}T\sum_n\int\frac{d^3k}{(2\pi)^3}\gamma_\mu\left[\tilde{\Delta}(i\tilde{\omega}_p-i\omega_n,\vec{p}-\vec{k})\mathcal{P}_R\cancel{K}\mathcal{P}_L\right]\gamma_\mu\Delta(i\omega_n,\vec{k}), \quad (4.1)$$

where  $\tilde{\Delta}(i\tilde{\omega}_p-i\omega_n,\vec{p}-\vec{k})$  and  $\Delta(i\omega_n,\vec{k})$  are defined in Eq. (A.1), and  $\mathcal{P}_{L(R)}$  denotes the left- and right-handed chiral projectors. Due to the unitarity of the CKM matrix, this contribution vanishes. Notably, this result agrees with those of the broken phase. Next, we analyze diagram (a), shown below

$$\begin{aligned} \Sigma_{u_L-c_L}^{(a)}(P) = & -T\sum_n\int\frac{d^3k}{(2\pi)^3}\lambda_{j'm'}^{d*}V_{m'1}^*\left[\tilde{\Delta}(i\tilde{\omega}_p-i\omega_n,\vec{p}-\vec{k})\mathcal{P}_R(\cancel{K}-\cancel{P})\delta_{jj'}\mathcal{P}_L\right] \\ & \times V_{2m}\lambda_{mj}^d\Delta\left(i\omega_n,\vec{k},\mu(T)\right), \end{aligned} \quad (4.2)$$

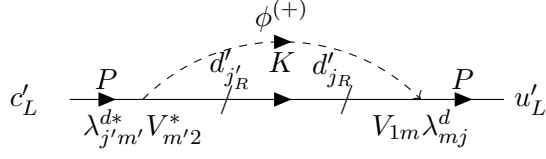


**Figure 5:** The Feynman diagram (in imaginary-time formalism) demonstrates the propagation of the left-handed charm quark to the up-quark.

where the coupling constant is

$$\lambda_{jm'}^{d*} V_{m'1}^* V_{2m} \lambda_{mj}^d = \lambda_{11}^{d*} V_{11}^* V_{21} \lambda_{11}^d + \lambda_{22}^{d*} V_{21}^* V_{22} \lambda_{22}^d + \lambda_{33}^{d*} V_{31}^* V_{23} \lambda_{33}^d \neq 0. \quad (4.3)$$

This manifestly demonstrates that at the one-loop order, flavor-changing effects through self-energies are possible. Following a similar approach to the calculations in Appendix (A), the self-energy in Eq. (4.2) is given by:

$$\Sigma_{u_L-c_L}^{(a)} = \left\{ \frac{m_{u_L-c_L}^2(T)}{|\vec{p}|} \gamma_0 \mathcal{Q}_0\left(\frac{p_0}{|\vec{p}|}\right) + \frac{m_{u_L-c_L}^2(T)}{|\vec{p}|} \vec{\gamma} \cdot \hat{p} \left[ 1 - \frac{p_0}{|\vec{p}|} \mathcal{Q}_0\left(\frac{p_0}{|\vec{p}|}\right) \right] \right\} \mathcal{P}_L, \quad (4.4)$$

where

$$m_{u_L-c_L}^2(T) = \frac{\lambda_{jm'}^{d*} V_{m'1}^* V_{2m} \lambda_{mj}^d T^2}{16}. \quad (4.5)$$

These off-diagonal self-energies violate  $CP$  because they do not involve the absolute values of the  $CP$ -violating matrices, in contrast to those calculated in the previous section. Most significantly, the rate of transition  $u_L$  to  $c_L$  is different from its counterpart:  $c_L$  to  $u_L$ . The thermal mass for the latter, which is shown in Fig.(5), is given

$$m_{c_L-u_L}^2(T) = \frac{\lambda_{jm'}^{d*} V_{m'2}^* V_{1m} \lambda_{mj}^d T^2}{16}. \quad (4.6)$$

The key differences between Eqs. (4.6) and (4.5) lie in the fact that the CKM matrix is not symmetric, for instance  $V_{11}^* V_{21} \neq V_{12}^* V_{11}$ . This demonstrates that there is an asymmetry between the propagation of  $u_L$  to  $c_L$  and  $c_L$  to  $u_L$ . The generalization of our results is illustrated in Fig. 6. For  $i = k$ , the results given by Eq. (3.8) are applicable, while for  $i \neq k$ , the results corresponding to flavor-changing processes are relevant, with the corresponding off-diagonal thermal masses given below

$$\begin{aligned} m_{u_{iL}-u_{kL}}^2(T) &= \frac{\lambda_{jm'}^{d*} V_{m'i}^* V_{km} \lambda_{mj}^d T^2}{16}, \\ m_{d_{iL}-d_{kL}}^2(T) &= \frac{\lambda_{jm'}^{u*} V_{m'i}^* V_{km}^* \lambda_{mj}^u T^2}{16}, \\ m_{\nu_{iL}-\nu_{kL}}^2(T) &= \frac{\lambda_{jm'}^{e*} U_{m'i}^* U_{km} \lambda_{mj}^e T^2}{16}, \\ m_{e_{iL}-e_{kL}}^2(T) &= \frac{\lambda_{jm'}^{\nu*} U_{m'i}^* U_{km}^* \lambda_{mj}^\nu T^2}{16}. \end{aligned} \quad (4.7)$$

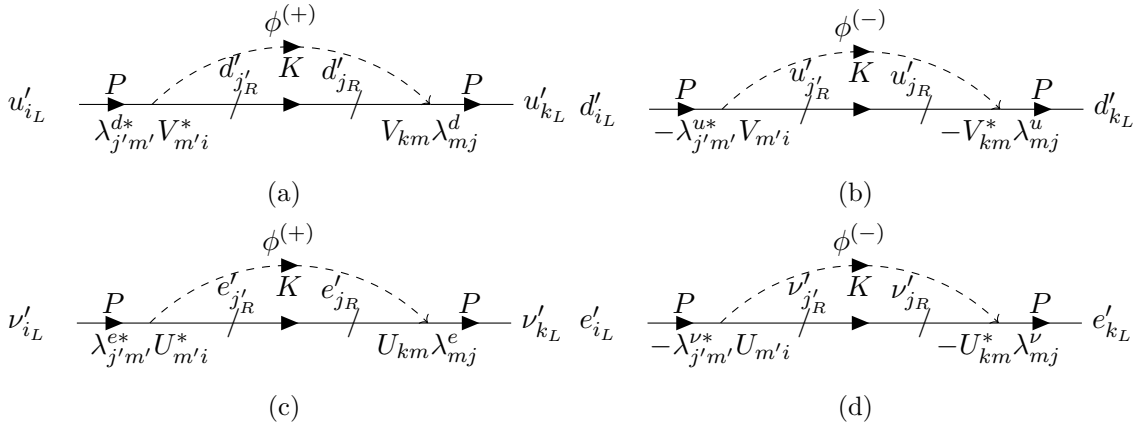


**Figure 6:** The Feynman diagrams (in the imaginary-time formalism) illustrate the propagation of the left-handed fermions for  $i \neq k$ .

From the relations above, we can define the matrix structure of thermal masses applicable to self-energies. For clarity, the matrix form of the thermal masses for left-handed up-quarks is presented below

$$M_{u_L}^2(T) = \frac{1}{16} \begin{pmatrix} 16m_{u_{1L}}^2(T) & \lambda_{jm'}^{d*} V_{m'1}^* V_{2m} \lambda_{mj}^d T^2 & \lambda_{jm'}^{d*} V_{m'1}^* V_{3m} \lambda_{mj}^d T^2 \\ \lambda_{jm'}^{d*} V_{m'2}^* V_{1m} \lambda_{mj}^d T^2 & 16m_{u_{2L}}^2(T) & \lambda_{jm'}^{d*} V_{m'2}^* V_{3m} \lambda_{mj}^d T^2 \\ \lambda_{jm'}^{d*} V_{m'3}^* V_{1m} \lambda_{mj}^d T^2 & \lambda_{jm'}^{d*} V_{m'3}^* V_{2m} \lambda_{mj}^d T^2 & 16m_{u_{3L}}^2(T) \end{pmatrix}, \quad (4.8)$$

where the diagonal thermal masses were acquired in Eq. (3.8). This non-diagonal matrix is caused by the non-diagonality of the Yukawa sector, which, due to the lack of degrees of freedom, cannot be fully diagonal. This is the main reason for the flavor changing of left-handed fermions in the symmetric phase. The key aspect of such propagations is that they do not occur at the tree level but instead emerge at the one-loop level. Because the off-diagonal components of CP-violating matrices are small, such propagations are small compared to diagonal ones. These propagations highlight the inability to define conventional propagators for left-handed fermions, necessitating exclusive analysis within the context of scattering processes. In contrast, as we mentioned before, the right-handed fermions retain their eigenstates, which we prove in the Appendix (B) explicitly.

At this stage, it is crucial to examine the theorem stating that "there is no FCNC" [54]. Its discussions have focused on the neutral Higgs sector, as only neutral Higgs bosons acquire vacuum expectation values in the Higgs mechanism [73]. However, its implications in the symmetric phase make clearer the origin of flavor-changing arising in the self-energies (or vertex diagrams). Since thermal masses emerge from one-loop corrections, both neutral and charged Higgs bosons—if present—contribute to thermal masses. While the zero temperature part can also enable flavor-changing processes, its finite renormalized contribution is negligible compared to the temperature-dependent part. This raises a key question: Why do one-loop self-energy and vertex corrections fail to induce flavor-changing processes in the broken phase? The answer lies in the FCNC theorem, which not only pre-



vents tree-level flavor-changing processes but also structures the Yukawa interactions such that self-energy and vertex corrections cannot induce flavor-changing phenomena. Hence, our main objective is to identify the mechanism permitting flavor-changing processes in the symmetric phase while forbidding them in the broken phase. Two key conditions from the FCNC theorem are highlighted below

- "The neutral current naturally conserves all quark flavors", requiring the Yukawa coupling matrix to be diagonal in the same basis as the quark mass matrix [54].
- Each right-handed fermion of a given charge ( $u_R$  or  $d_R$ ) must couple to only one Higgs boson, a condition automatically satisfied in the broken phase of the SM and MESM.

In the broken phase, these conditions prevent, for instance, the following Yukawa interaction, [74]:

$$\bar{u}_{iL} \left[ f_{ij}^1 \phi_1^{(0)} + f_{ij}^2 \phi_2^{(0)} \right] u_{jR} + H.C, \quad (4.9)$$

where  $f_{ij}^{1,2}$  are Yukawa coupling constants, and  $\phi_{1,2}^{(0)}$  are considered as the neutral Higgs bosons with the vacuum expectation values  $\langle \phi_{1,2}^{(0)} \rangle = \frac{v_{1,2}}{\sqrt{2}}$ . As discussed before, only one of these coupling constants can be fully diagonalized, while the other induces FCNCs not only through self-energy and vertex corrections but also at the tree level through the Higgs mechanism, in the broken phase<sup>6</sup>. Conversely, in the symmetric phase, in which the Higgs expectation value vanishes, the flavor-changing phenomenon is enabled at the one-loop order in both self-energies and vertex diagrams. As a result, simultaneous diagonalization of both Yukawa coupling matrices is impossible, contradicting the first condition. Additionally, The right-handed fermions interact with  $\phi^{(+)}$  and  $\phi^{(0)}$ , violating the second FCNC condition. As discussed in Sec (1), the constraints of FCNC and GIM mechanisms ensure that in the broken phase, flavor-changing processes only appear in the box diagrams.

Finally, the finite-temperature fermion propagators at the one-loop order, ignoring zero-temperature contributions, are:

$$\begin{aligned} S_{f_{iL}}(P) &= \left\{ \frac{i}{\not{P}} - \frac{i}{\not{P}} \Sigma_{f_{iL}}^T \frac{1}{\not{P}} \right\} \mathcal{P}_L \approx \left\{ \frac{i}{\not{P} - \Sigma_{f_{iL}}^T} \right\} \mathcal{P}_L, \\ S_{f_{iR}}(P) &= \left\{ \frac{i}{\not{P}} - \frac{i}{\not{P}} \Sigma_{f_{iR}}^T \frac{1}{\not{P}} \right\} \mathcal{P}_R \approx \left\{ \frac{i}{\not{P} - \Sigma_{f_{iR}}^T} \right\} \mathcal{P}_R, \\ S_{f_{iL} - f_{kL}}(P) &= \left\{ -\frac{i}{\not{P}} \Sigma_{f_{iL} - f_{kL}}^T \frac{1}{\not{P}} \right\} \mathcal{P}_L, \end{aligned} \quad (4.10)$$

where  $f_{iL,R}$  represents fermion propagators with identical particles in the initial and final states, and  $f_{iL} - f_{kL}$  represents flavor transformations specific to left-handed fermions in which  $i \neq k$ .

---

<sup>6</sup>For more explanations, refer to Ref. [74]

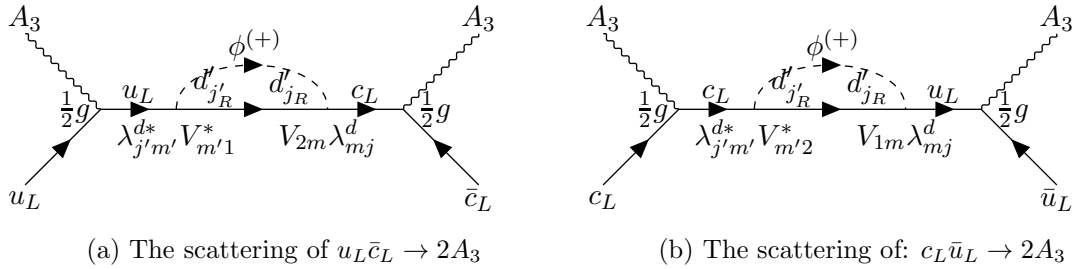


**Figure 7:** Possible scattering processes of  $u_L$  and  $c_L$  (in imaginary-time).

## 5 The Scattering Processes

In this section, we summarize the possible scattering processes induced by flavor-changing interactions in the self-energies, such as  $u_L \bar{c}_L \rightarrow 2A_3$ , which are illustrated in Fig. (7)(a), highlighting the novel phenomena unique to the symmetric phase. Notably, the analogous scattering  $c_L \bar{u}_L \rightarrow 2A_3$ , shown in Fig. (7)(b), yields different outcomes due to the different contributions from its self-energy. Furthermore, the inverse of these processes can also occur, i.e., for instance,  $B_Y + A_3 \rightarrow u_L \bar{c}_L$ , and  $B_Y + A_3 \rightarrow u_L \bar{c}_L$ , within the different probabilities. Analogous scattering can also occur for the other left-handed fermions, illustrated in Fig. (8). However, these processes arise at one-loop diagrams along within off-diagonal components of CP-violating matrices. This significantly reduces the impact of such processes in scenarios where tree-level or even one-loop diagrams (with diagonal components of CP-violating matrices or with gauge coupling constants) exist. These processes further highlight the importance of focusing on interactions where neutral gauge fields and different flavors of fermions contribute. These might impact the scenarios in which CP violation is considered, but we postpone it to other studies.

## 6 Summary and Conclusion

In this study, expressing the MESM in the mass basis, neglecting the zero temperature part and assuming the effective Higgs masses are negligible compared to temperature, the self-energy  $\Sigma_T$  was written in the high-temperature limit, revealing the emergence of thermal masses. In the latter, the absolute values of CP-violating components appeared in the Yukawa contributions for left-handed fermions. In contrast, in the Yukawa contributions for right-handed fermions or weak interactions, the components of CP-violating matrices did not contribute. Subsequently, these results were reduced to SM, in which the results for the CKM matrix only became relevant. Additionally, we discussed that considering the high-temperature limit in the broken phase is incorrect due to large three-level masses of top-quark, the weak gauge bosons, and the Higgs boson.

Next, we explicitly demonstrated how the lack of degrees of freedom to fully diagonalize the Yukawa sectors makes the flavor-changing processes an inevitable feature of the symmetric phase, occurring at the one-loop level. In this case, the two conditions of FCNC are violated naturally in the symmetric phase, confirming our conclusion. Although the CP violation also exists in the broken phase through box diagrams, preserving the diagonal

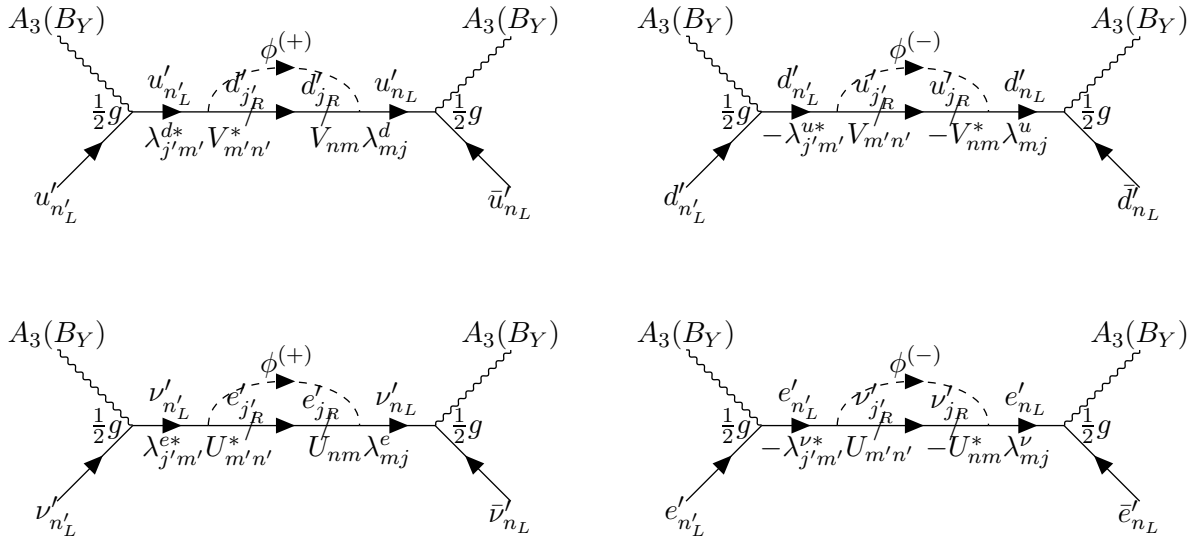


**Figure 8:** The possible scatterings for different generation of left-handed fermions with  $n \neq n'$  including the processes  $f'_{n'_L} \bar{f}'_{n_L} \rightarrow 2A_3$ ,  $f'_{n'_L} \bar{f}'_{n_L} \rightarrow 2B_Y$ ,  $f'_{n'_L} \bar{f}'_{n_L} \rightarrow A_3 + B_Y$ . Here,  $f'_{n_L} \bar{f}'_{n_L}$  denotes the process for different flavors of the same charged particle.

form of propagators, we can define the particles with their unique mass and self-energies arising in the pole of the propagators. Here, we are faced with a different issue, indicating that not only the flavor of the left-handed fermions violates but also it can occur through the off-diagonal self-energies: For instance, the left-handed up-quark can propagate to the left-handed charm quark. These phenomena can reinforce the CP-violating processes in the Early Universe because, in addition to box diagrams, they occur in the self-energies. However, these are suppressed compared to processes preserving CP. First of all, they occur at one-loop order corrections, and second, the off-diagonal components of the CP-violating matrices emerge, which are significantly smaller than diagonal components. The latter only appears where the flavor of particles is preserved: For instance, the propagation of left-handed up-quarks to itself is much larger than their propagations to left-handed charm quarks. Finally, we explored novel scattering processes, highlighting the unique CP-violating effects of the symmetric phase. These findings may reshape our understanding of CP violation in the Early Universe.

## Appendices

### A Thermal Mass Calculations

In this appendix, we calculate the thermal masses in the symmetric phase using the imaginary-time formalism and HTL approximation. For simplicity, we first focus on the left-handed up quarks, including their electroweak interactions (see Eq. (3.7)); We then take strong interactions into account. For the first case, the corresponding Feynman dia-

grams in the imaginary-time formalism (Euclidean space-time with finite interval  $\beta$  [2]) are shown in Figure (2). This appendix follows the approach in Ref. [2], where calculations were performed for massless Quantum Electrodynamics (QED) and massless SU(N) gauge theories with massless gauge fields. However, due to the significance of the Higgs effective masses in the symmetric phase, the discussions related to the broken phase, and most importantly, calculations of flavor-changing in self-energies, we are motivated to extend these calculations to at least the left-handed up quarks, which includes all relevant interactions. Later, we extend these to flavor-changing processes. The tree-level propagators for left-, right-handed fermions, gauge bosons, and massive scalars, in imaginary-time formalism, are given below, respectively

$$\begin{aligned}
S_L(i\tilde{\omega}_n, \vec{p}) &= \mathcal{P}_L \frac{-\not{P} \delta_{ij}}{P^2} \mathcal{P}_R \equiv -\tilde{\Delta}(i\tilde{\omega}_n, \vec{p}) \mathcal{P}_L \not{P} \delta_{ij} \mathcal{P}_R, \\
S_R(i\tilde{\omega}_n, \vec{p}) &= \mathcal{P}_R \frac{-\not{P} \delta_{ij}}{P^2} \mathcal{P}_L \equiv -\tilde{\Delta}(i\tilde{\omega}_n, \vec{p}) \mathcal{P}_R \not{P} \delta_{ij} \mathcal{P}_L, \\
\Delta^{\mu\nu}(i\omega_n, \vec{p}) &= \frac{\delta^{\mu\nu}}{P^2} \equiv \Delta(i\omega_n, \vec{p}) \delta^{\mu\nu}, \\
\Delta(i\omega_n, \vec{p}, \mu) &= \frac{1}{P^2 + \mu^2},
\end{aligned} \tag{A.1}$$

where  $P^2 = \tilde{\omega}^2 + \vec{p}^2$  for fermion propagator,  $P^2 = \omega^2 + \vec{p}^2$  for boson propagator,  $\not{P} = -\omega_n \gamma^4 + \vec{k} \cdot \vec{\gamma}$ <sup>7</sup>, and  $\mathcal{P}_L$  ( $\mathcal{P}_R$ ) is the left-handed (right-handed) chiral projector which is  $\frac{1-\gamma^5}{2}$  ( $\frac{1+\gamma^5}{2}$ ). Furthermore, there is an important relation in imaginary-time formalism<sup>8</sup> for both fermionic and bosonic free propagators given below [2]

$$\Delta(i\omega_n, E_p) = \frac{1}{\omega_n^2 + E_p^2} = \sum_{s=\pm} \Delta_s(i\omega_n, E_p) = \sum_{s=\pm} \frac{-s}{2E_p} \frac{1}{i\omega_n - sE_p}, \tag{A.2}$$

where, in the case of the fermion propagator,  $\omega$  is replaced with  $\tilde{\omega}$ , as is  $\Delta$ .

Now let us compute the self-energy of the diagram (a) in imaginary-time formalism

---

<sup>7</sup>We used the conventions of Ref. [2], where the analytical continuation from Euclidean to Minkowski space-time is performed by applying the transformations  $\gamma^4 \rightarrow i\gamma^0$ ,  $i\omega_n \rightarrow q_0$ , and  $\vec{k} \cdot \vec{p} \rightarrow -\vec{k} \cdot \vec{p}$ . Here,  $\gamma^0$  represents the Dirac matrix in the Minkowski space-time.

<sup>8</sup>We use these relations in calculations of one-loop propagators.

presented below<sup>9</sup>

$$\begin{aligned}
\Sigma_{u_{iL}}^{(a)}(P) &= -T \sum_n \int \frac{d^3k}{(2\pi)^3} \lambda_{j'm'}^{d*} V_{m'i}^* \left[ \tilde{\Delta}(i\tilde{\omega}_p - i\omega_n, \vec{p} - \vec{k}) \mathcal{P}_R (\not{K} - \not{P}) \delta_{jj'} \mathcal{P}_L \right] \\
&\quad \times V_{im} \lambda_{mj}^d \Delta(i\omega_n, \vec{k}, \mu(T)) \\
&= -|V_{ij} \lambda^{d_j}|^2 T \sum_n \int \frac{d^3k}{(2\pi)^3} \left[ \tilde{\Delta}(i\tilde{\omega}_p - i\omega_n, \vec{p} - \vec{k}) \mathcal{P}_R (\not{K} - \not{P}) \mathcal{P}_L \right] \Delta(i\omega_n, \vec{k}, \mu(T)) \\
&\approx -|V_{ij} \lambda^{d_j}|^2 \left\{ T \sum_n \int \frac{d^3k}{(2\pi)^3} \tilde{\Delta}(i\tilde{\omega}_p - i\omega_n, \vec{p} - \vec{k}) \not{K} \Delta(i\omega_n, \vec{k}, \mu(T)) \right\} \mathcal{P}_L, \\
&= -|V_{ij} \lambda^{d_j}|^2 \left\{ T \sum_n \int \frac{d^3k}{(2\pi)^3} \tilde{\Delta}(i\tilde{\omega}_p - i\omega_n, \vec{p} - \vec{k}) \not{K} \Delta(i\omega_n, \vec{k}, \mu(T)) \right\} \mathcal{P}_L,
\end{aligned} \tag{A.3}$$

in which we used, respectively, the diagonality of Yukawa coupling constants, properties of chiral projectors, and neglecting  $\not{P}$  compared to  $\not{K}$ . Furthermore, ‘ $i$ ’ is generation index (not Einstein summation), and  $\tilde{\omega}_p$  and  $\omega_n$  are the discrete energies for external momentum  $P$  and internal momentum  $K$ , respectively. Here, the coupling constant is precisely

$$|V_{ij} \lambda^{d_j}|^2 = |V_{i1} \lambda^d|^2 + |V_{i2} \lambda^c|^2 + |V_{i3} \lambda^b|^2. \tag{A.4}$$

To perform the sum of internal frequencies<sup>10</sup>, we can use the formula presented below [2]

$$\begin{aligned}
\mathcal{I}_1 &\equiv T \sum_n \omega_n \Delta(i\omega_n, E_1) \tilde{\Delta}(i(\tilde{\omega}_p - \omega_n), E_2) \\
&= T \sum_n \sum_{s_1, s_2 = \pm 1} \omega_n \Delta_{s_1}(i\omega_n, E_1) \tilde{\Delta}_{s_2}(i(\tilde{\omega}_p - \omega_n), E_2) \\
&= \sum_{s_1, s_2 = \pm 1} \frac{is_2}{4E_2} \frac{1 + f(s_1 E_1) - \tilde{f}(s_2 E_2)}{i\tilde{\omega}_p - s_1 E_1 - s_2 E_2},
\end{aligned} \tag{A.5}$$

and

$$\begin{aligned}
\mathcal{I}_2 &\equiv T \sum_n \Delta(i\omega_n, E_1) \tilde{\Delta}(i(\tilde{\omega}_p - \omega_n), E_2) \\
&= T \sum_n \sum_{s_1, s_2 = \pm 1} \Delta_{s_1}(i\omega_n, E_1) \tilde{\Delta}_{s_2}(i(\tilde{\omega}_p - \omega_n), E_2) \\
&= - \sum_{s_1, s_2 = \pm 1} \frac{s_1 s_2}{4E_1 E_2} \frac{1 + f(s_1 E_1) - \tilde{f}(s_2 E_2)}{i\tilde{\omega}_p - s_1 E_1 - s_2 E_2},
\end{aligned} \tag{A.6}$$

---

<sup>9</sup>Note that, in conventions which are utilized, the fermion self-energy is defined as the negative of its Feynman diagram [2].

<sup>10</sup>In the imaginary-time formalism, the continuous energy in conventional QFT changes into a discrete one due to finite interval time.

in which

$$\begin{aligned} \tilde{f}(E_2) &= \tilde{n}(E_2), & f(E_1) &= n(E_1), \\ \tilde{f}(-E_2) &= 1 - \tilde{n}(E_2), & f(E_1) &= -1 - n(E_1), \end{aligned} \quad (\text{A.7})$$

where  $n(E)$  and  $\tilde{n}(E)$  are Bose-Einstein and Fermi-Dirac distribution functions, respectively. Using these equations the curly bracket in (A.3) becomes as [2]

$$\begin{aligned} -T \sum_n \int \frac{d^3k}{(2\pi)^3} \gamma_4 \omega_n \tilde{\Delta}(i\omega_p - i\omega_n, \vec{p} - \vec{k}) \Delta(i\omega_n, \vec{k}, \mu(T)) &= \frac{-\gamma_4}{8\pi^2} \int \frac{k^2 dk d\Omega}{4\pi} \frac{i}{E_2} \\ &\times [(1 + n(E_1) - \tilde{n}(E_2)) \left( \frac{1}{i\tilde{\omega}_p - E_1 - E_2} + \frac{1}{i\tilde{\omega}_p + E_1 + E_2} \right) \\ &- (n(E_1) + \tilde{n}(E_2)) \left( \frac{1}{i\tilde{\omega}_p + E_1 - E_2} + \frac{1}{i\tilde{\omega}_p - E_1 + E_2} \right)], \end{aligned} \quad (\text{A.8})$$

and

$$\begin{aligned} T \sum_n \int \frac{d^3k}{(2\pi)^3} \vec{\gamma} \cdot \vec{k} \tilde{\Delta}(i\omega_p - i\omega_n, \vec{p} - \vec{k}) \Delta(i\omega_n, \vec{k}, \mu(T)) &= \frac{-\gamma_i}{8\pi^2} \int \frac{k^2 dk d\Omega}{4\pi} k \hat{k}_i \frac{1}{E_1 E_2} \\ &\times [(1 + n(E_1) - \tilde{n}(E_2)) \left( \frac{1}{i\tilde{\omega}_p - E_1 - E_2} - \frac{1}{i\tilde{\omega}_p + E_1 + E_2} \right) \\ &+ (n(E_1) + \tilde{n}(E_2)) \left( \frac{1}{i\tilde{\omega}_p + E_1 - E_2} - \frac{1}{i\tilde{\omega}_p - E_1 + E_2} \right)], \end{aligned} \quad (\text{A.9})$$

where  $E_1 = \sqrt{\vec{k}^2 + \mu^2(T)}$ ,  $E_2 = |\vec{p} - \vec{k}|$ . Applying HTL, we can write

$$\begin{aligned} E_1 &= \sqrt{k^2 + \mu^2(T)} \approx k, \\ E_2 &= \sqrt{k^2 + p^2 - 2kp \cos(\theta)} \approx k - p \cos(\theta), \\ n(E_1) &\approx n(k), \\ \tilde{n}(E_2) &= \tilde{n}(|\vec{k} - \vec{p}|) \approx \tilde{n}(k) - p \cos(\theta) \frac{d\tilde{n}(k)}{dk}. \end{aligned} \quad (\text{A.10})$$

Here  $\mu^2(T) \approx c^2 + \pi(0)$  in which  $c^2$  is negative square mass written in conventional QFT for SM (or MESM), and  $\pi(0)$  demonstrates Higgs fields self-energy acquired using the effective potential approach, encompasses the electroweak coupling constants. At the leading order,  $\pi(0) = \xi^2 T^2$ , where  $\xi$  denotes the order of coupling constant, but for finding the precise relation (for SM), one can infer to Ref. [22]. The only contribution concerning us is the top-quark one:  $\pi = \frac{1}{4} |\lambda^t|^2 T^2$ , where  $\lambda^t \approx 1$ . However, negative mass squared  $c^2$  along with the coefficient  $\frac{1}{4}$  can make us confident that  $\mu(T)$  is negligible compared to temperature. Furthermore the external three-momentum  $|\vec{p}|$  is order of  $\eta T$ , where  $\eta$  denotes the coupling constant. Hence  $|\vec{p}|$  and  $\mu(T)$  are negligible compared to  $|\vec{k}|$ . Utilizing Eq. (A.10), the temperature-dependent terms, which include the Bose-Einstein or Fermi-Dirac distributions, in the first line of Eq. (A.8) and (A.9) result in order of  $T$  [2, 60], while the second term of Eqs. (A.8) and (A.9) are order of  $T^2$ . Thus, because the high-temperature limit is

considered, the first one is negligible compared to the second one. Furthermore, the terms that do not contain Bose-Einstein or Fermi-Dirac distributions are proportional to zero-temperature (or conventional QFT vacuum), which can be renormalized and are ignored in this study. At this stage, using the equations presented below

$$\int_0^\infty k \, dk n(k) = 2 \int_0^\infty k \, dk \tilde{n}(k) = \frac{\pi^2 T^2}{6}, \quad (\text{A.11})$$

the Eqs. (A.8) and (A.9) are derived as

$$\begin{aligned} -T \sum_n \int \frac{d^3 k}{(2\pi)^3} \gamma_4 \omega_n \tilde{\Delta}(i\tilde{\omega}_p - i\omega_n, \vec{p} - \vec{k}) \Delta(i\omega_n, \vec{k}, \mu(T)) &\simeq \frac{T^2}{16} \int \frac{d\Omega}{4\pi} \frac{i\gamma_4}{i\tilde{\omega}_p + p \cos(\theta)}, \\ T \sum_n \int \frac{d^3 k}{(2\pi)^3} \vec{\gamma} \cdot \vec{k} \tilde{\Delta}(i\tilde{\omega}_p - i\omega_n, \vec{p} - \vec{k}) \Delta(i\omega_n, \vec{k}, \mu(T)) &\simeq \frac{-T^2}{16} \int \frac{d\Omega}{4\pi} \frac{\gamma \cdot \hat{k}}{i\tilde{\omega}_p + p \cos(\theta)}. \end{aligned} \quad (\text{A.12})$$

Hence, replacing Eq. (A.12) in Eq. (A.3), the self-energy in the imaginary time (Euclidean space-time) can be written

$$\Sigma_{u_{iL}}^{(a)}(P) \simeq \left\{ m_{u_{iL}}^2(T) \int \frac{d\Omega}{4\pi} \frac{\hat{K}}{P \cdot \hat{K}} \right\} \mathcal{P}_L, \quad (\text{A.13})$$

where  $m_{u_{iL}}^2(T) = \frac{|V_{ij}\lambda^{d_j}|^2 T^2}{16}$ ,  $\hat{K} \equiv (-i, \hat{k})$ ,  $\mathbb{K} = -i\gamma^4 + \vec{\gamma} \cdot \vec{p}$ ,  $\hat{K} \cdot P = i\omega + \vec{k} \cdot \vec{p}$  and the symbol  $\simeq$  used for demonstrate the HTL in addition to ignoring zero temperature part. As a consequence, using analytical continuation from Euclidean to Minkowski space-time [2],  $\gamma_4 \rightarrow i\gamma_0$ ,  $\vec{p} \cdot \vec{k} \rightarrow -\vec{p} \cdot \vec{k}$ ,  $i\omega \rightarrow p_0$ , and perform the integration, the retarded self-energy (in Minkowski space-time) can be derived as [2]

$$\Sigma_{u_{iL}}^{(a)} = \left\{ \frac{m_{u_{iL}}^2(T)}{|\vec{p}|} \gamma_0 \mathcal{Q}_0\left(\frac{p_0}{|\vec{p}|}\right) + \frac{m_{u_{iL}}^2(T)}{|\vec{p}|} \vec{\gamma} \cdot \hat{p} \left[ 1 - \frac{p_0}{|\vec{p}|} \mathcal{Q}_0\left(\frac{p_0}{|\vec{p}|}\right) \right] \right\} \mathcal{P}_L, \quad (\text{A.14})$$

where  $\mathcal{Q}_0\left(\frac{p_0}{|\vec{p}|}\right)$  have been introduced in Eq. ((3.4)). Here, (a) indicates the contribution of the diagram (a) to the thermal mass of the left-handed up-quarks. Comparably, the self-energies of diagrams (b) to (e) similar to Eq. (A.14) are obtained, a primary difference in their thermal mass contributions, which can be derived as

$$\begin{aligned} m_{u_{iL}}^{(b)}(T) &= \frac{|\lambda^{u_i}|^2 T^2}{16}, & m_{u_{iL}}^{(c)}(T) &= \frac{1}{32} g^2 T^2, \\ m_{u_{iL}}^{(d)}(T) &= \frac{g'^2 T^2}{288}, & m_{u_{iL}}^{(e)}(T) &= \frac{1}{16} V_{ij} V_{ji}^* g^2 T^2 = \frac{2}{32} g^2 T^2. \end{aligned} \quad (\text{A.15})$$

where, in the last term, the unitarity of the CKM matrix is used. Furthermore, the

contribution of  $SU(3)$  interactions to quarks is given as [2]

$$m_q^2(T) = \frac{g'^2 T^2}{6}. \quad (\text{A.16})$$

As a consequence, the final thermal masses of the left-handed up-quarks are the sum of all these contributions, written in Eq. (3.8).

Analogously, the differences for the self-energy of  $u_{iR}$  (see Fig. (3)) lie in thermal masses along with chiral projectors. For instance, the thermal mass of diagram (a) is given

$$m_{u_{iR}}^2(T) = \frac{\lambda_{im}^{u*} V_{mj} V_{jm'}^* \lambda_{m'i}^u T^2}{16} = \frac{|\lambda^{u_i}|^2 T^2}{16}, \quad (\text{A.17})$$

where the diagonality of Yukawa coupling constants and unitarity of the CKM matrix are used. The remaining thermal masses in Fig. (3) can be derived similarly, and the final result is written in Eq. (3.8).

## B Proof of the Absence of Flavor-Changing Processes for the Right-Handed Fermions

In this appendix, we aim to demonstrate that no flavor-changing occurs for right-handed fermions. For completeness, we focus on the Leptons' Lagrangian in this analysis, which, similar to Eq. (3.7), is expanded below

$$\begin{aligned} \mathcal{L}'_{Leptons} = & i\bar{\nu}'_{iL} \left( \not{\partial} + \frac{ig}{2} \mathcal{A}_3 - \frac{i}{2} g' \not{\mathcal{B}}_Y \right) \nu'_{iL} + i\bar{\nu}'_{iL} \left( U_{ij} \frac{ig}{2} (\mathcal{A}_1 - i\mathcal{A}_2) \right) d'_{jL} \\ & + i\bar{e}'_{iL} \left( U_{ij}^* \left( \frac{ig}{2} (\mathcal{A}_1 + i\mathcal{A}_2) \right) \right) \nu'_{jL} + i\bar{e}'_{iL} \left( \not{\partial} - \frac{ig}{2} \mathcal{A}_3 + \frac{i}{2} g' \not{\mathcal{B}}_Y \right) e'_{iL} \\ & + i\bar{e}'_{iR} \left( \not{\partial} - \frac{i}{2} g' \not{\mathcal{B}}_Y \right) e'_{iR} + \bar{\nu}_{iR} \not{\partial} \nu_{iR} \\ & - \left\{ \bar{\nu}'_{iL} U_{im} \lambda_{mj}^e \phi^{(+)} e'_{jR} + \bar{e}'_{iL} \lambda_{ij}^e \phi^{(0)} e'_{jR} \right\} - H.C. \\ & - \left\{ \bar{\nu}'_{iL} \lambda_{ij}^\nu \phi^{(0)*} \nu'_{jR} - \bar{e}'_{iL} U_{im}^* \lambda_{mj}^\nu \phi^{(+)*} \nu'_{jR} \right\} - H.C. \end{aligned} \quad (\text{B.1})$$

For simplicity, we focus on the transition of  $\nu'_{iR}$  to  $\nu'_{kR}$ , which the  $\phi^{(+)}$  sector is responsible for activating flavor transformation (See Fig. (9)). Analogous to Eq (4.4), the right-handed self-energy only differs in chiral projector and its thermal masse presented below

$$m_{\nu'_{iR} - \nu'_{kR}}^2(T) = \frac{\lambda_{im'}^\nu U_{m'j}^* U_{jm} \lambda_{mk}^{\nu*}}{16} T^2 = 0, \quad (\text{B.2})$$

where the diagonality of Yukawa coupling constants and unitarity of the PMNS matrix is used. This result can easily be generalized to the entire right-handed fermions.



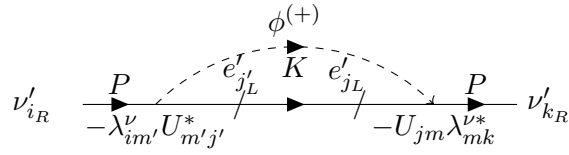


**Figure 9:** The Feynman diagram (in imaginary-time formalism) demonstrates the propagation of the right-handed neutrinos.

## References

- [1] J.I. Kapusta and C. Gale, *Finite-temperature field theory: Principles and applications*, Cambridge Monographs on Mathematical Physics, Cambridge University Press (2011), [10.1017/CBO9780511535130](https://doi.org/10.1017/CBO9780511535130).
- [2] M.L. Bellac, *Thermal Field Theory*, Cambridge Monographs on Mathematical Physics, Cambridge University Press (3, 2011), [10.1017/CBO9780511721700](https://doi.org/10.1017/CBO9780511721700).
- [3] M. Laine and A. Vuorinen, *Basics of Thermal Field Theory*, vol. 925, Springer (2016), [10.1007/978-3-319-31933-9](https://doi.org/10.1007/978-3-319-31933-9), [[1701.01554](https://arxiv.org/abs/1701.01554)].
- [4] M.G. Mustafa, *An introduction to thermal field theory and some of its application*, *Eur. Phys. J. ST* **232** (2023) 1369 [[2207.00534](https://arxiv.org/abs/2207.00534)].
- [5] H. Leutwyler and S. Mallik, *Finite temperature scalar field theory in the early universe*, *Annals of Physics* **205** (1991) 1.
- [6] A.H. Guth and S.H.H. Tye, *Phase transitions and magnetic monopole production in the very early universe*, *Phys. Rev. Lett.* **44** (1980) 631.
- [7] S. Hawking and I. Moss, *Supercooled phase transitions in the very early universe*, *Physics Letters B* **110** (1982) 35.
- [8] A. Schenk, *Pion propagation at finite temperature*, *Phys. Rev. D* **47** (1993) 5138.
- [9] M. Quiros, *Finite temperature field theory and phase transitions*, in *ICTP Summer School in High-Energy Physics and Cosmology*, pp. 187–259, 1, 1999 [[hep-ph/9901312](https://arxiv.org/abs/hep-ph/9901312)].
- [10] A. Ekstedt and J. Löfgren, *A Critical Look at the Electroweak Phase Transition*, *JHEP* **12** (2020) 136 [[2006.12614](https://arxiv.org/abs/2006.12614)].
- [11] N. Landsman and C. van Weert, *Real- and imaginary-time field theory at finite temperature and density*, *Physics Reports* **145** (1987) 141.
- [12] T. Matsubara, *A New approach to quantum statistical mechanics*, *Prog. Theor. Phys.* **14** (1955) 351.
- [13] Y. Takahashi and H. Umezawa, *Thermo field dynamics*, *Int. J. Mod. Phys. B* **10** (1996) 1755.
- [14] P. Higgs, *Broken symmetries, massless particles and gauge fields*, *Physics Letters* **12** (1964) 132.
- [15] P.W. Higgs, *Spontaneous symmetry breakdown without massless bosons*, *Phys. Rev.* **145** (1966) 1156.
- [16] P.W. Higgs, *Broken symmetries and the masses of gauge bosons*, *Phys. Rev. Lett.* **13** (1964) 508.

- [17] D.A. Kirzhnits and A.D. Linde, *Macroscopic Consequences of the Weinberg Model*, *Phys. Lett. B* **42** (1972) 471.
- [18] L. Dolan and R. Jackiw, *Symmetry behavior at finite temperature*, *Phys. Rev. D* **9** (1974) 3320.
- [19] S. Weinberg, *Gauge and global symmetries at high temperature*, *Phys. Rev. D* **9** (1974) 3357.
- [20] D.A. Kirzhnits and A.D. Linde, *Symmetry Behavior in Gauge Theories*, *Annals Phys.* **101** (1976) 195.
- [21] A.D. Linde, *Phase transitions in gauge theories and cosmology*, *Reports on Progress in Physics* **42** (1979) 389.
- [22] M.E. Carrington, *Effective potential at finite temperature in the standard model*, *Phys. Rev. D* **45** (1992) 2933.
- [23] A. Katz and M. Perelstein, *Higgs couplings and electroweak phase transition*, *Journal of High Energy Physics* **2014** (2014) .
- [24] I. Baldes, T. Konstandin and G. Servant, *A first-order electroweak phase transition from varying yukawas*, *Physics Letters B* **786** (2018) 373.
- [25] S. Davidson, K. Kainulainen and K. Olive, *Protecting the baryon asymmetry with thermal masses*, *Physics Letters B* **335** (1994) 339–344.
- [26] D. Bödeker and W. Buchmüller, *Baryogenesis from the weak scale to the grand unification scale*, *Rev. Mod. Phys.* **93** (2021) 035004.
- [27] R. Baier, B. Pire and D. Schiff, *Dilepton production at finite temperature: Perturbative treatment at order  $\alpha_s$* , *Phys. Rev. D* **38** (1988) 2814.
- [28] P. Arnold, G.D. Moore and L.G. Yaffe, *Photon emission from quark-gluon plasma: complete leading order results*, *Journal of High Energy Physics* **2001** (2001) 009–009.
- [29] M.G. Mustafa, M.H. Thoma and P. Chakraborty, *Screening of a moving parton in the quark-gluon plasma*, *Physical Review C* **71** (2005) .
- [30] M.G. Mustafa, P. Chakraborty and M.H. Thoma, *Dynamical screening in a quark gluon plasma*, *Journal of Physics: Conference Series* **50** (2006) 438–441.
- [31] P. Chakraborty, M.G. Mustafa and M.H. Thoma, *Wakes in the quark-gluon plasma*, *Physical Review D* **74** (2006) .
- [32] R.D. Pisarski, *Damping rates for moving particles in hot qcd*, *Phys. Rev. D* **47** (1993) 5589.
- [33] S. Peigné, E. Pilon and D. Schiff, *The heavy fermion damping rate puzzle*, *Zeitschrift für Physik C Particles and Fields* **60** (1993) 455–460.
- [34] M.H. Thoma, *Damping rate of a hard photon in a relativistic plasma*, *Phys. Rev. D* **51** (1995) 862.
- [35] E. Braaten and R.D. Pisarski, *Resummation and gauge invariance of the gluon damping rate in hot qcd*, *Phys. Rev. Lett.* **64** (1990) 1338.
- [36] G.S. Rocha and G.S. Denicol, *Transport coefficients of transient hydrodynamics for the hadron-resonance gas and thermal-mass quasiparticle models*, *Phys. Rev. D* **109** (2024) 096011.
- [37] N. Chakraborty, P. Konar, R. Roshan and S. Show, *Thermally corrected masses and freeze-in dark matter: A case study*, *Phys. Rev. D* **107** (2023) 035021.

- [38] N. Bernal, K. Deka and M. Losada, *Thermal dark matter with low-temperature reheating*, 2024.
- [39] G. Arcadi, N. Benincasa, A. Djouadi and K. Kannike, *The  $2hd+a$  model: collider, dark matter and gravitational wave signals*, 2023.
- [40] E. Braaten and R.D. Pisarski, *Simple effective lagrangian for hard thermal loops*, *Phys. Rev. D* **45** (1992) R1827.
- [41] E. Braaten and R.D. Pisarski, *Deducing hard thermal loops from ward identities*, *Nuclear Physics B* **339** (1990) 310.
- [42] J.C. Taylor and S.M.H. Wong, *The Effective Action of Hard Thermal Loops in QCD*, *Nucl. Phys. B* **346** (1990) 115.
- [43] J. Frenkel and J. Taylor, *Hard thermal qcd, forward scattering and effective actions*, *Nuclear Physics B* **374** (1992) 156.
- [44] J.O. Andersen, E. Braaten and M. Strickland, *Hard-thermal-loop resummation of the free energy of a hot gluon plasma*, *Phys. Rev. Lett.* **83** (1999) 2139.
- [45] J.O. Andersen, E. Braaten, E. Petitgirard and M. Strickland, *Hard-thermal-loop perturbation theory to two loops*, *Phys. Rev. D* **66** (2002) 085016.
- [46] J.O. Andersen, L.E. Leganger, M. Strickland and N. Su, *Three-loop htl qcd thermodynamics*, *Journal of High Energy Physics* **2011** (2011) .
- [47] N. Haque, A. Bandyopadhyay, J.O. Andersen, M.G. Mustafa, M. Strickland and N. Su, *Three-loop htlpt thermodynamics at finite temperature and chemical potential*, *Journal of High Energy Physics* **2014** (2014) .
- [48] N. Haque, J.O. Andersen, M.G. Mustafa, M. Strickland and N. Su, *Three-loop pressure and susceptibility at finite temperature and density from hard-thermal-loop perturbation theory*, *Phys. Rev. D* **89** (2014) 061701.
- [49] N. Cabibbo, *Unitary Symmetry and Leptonic Decays*, *Phys. Rev. Lett.* **10** (1963) 531.
- [50] M. Kobayashi and T. Maskawa, *CP Violation in the Renormalizable Theory of Weak Interaction*, *Prog. Theor. Phys.* **49** (1973) 652.
- [51] B. Pontecorvo, *Inverse beta processes and nonconservation of lepton charge*, *Zh. Eksp. Teor. Fiz.* **34** (1957) 247.
- [52] Z. Maki, M. Nakagawa and S. Sakata, *Remarks on the unified model of elementary particles*, *Prog. Theor. Phys.* **28** (1962) 870.
- [53] S.L. Glashow, J. Iliopoulos and L. Maiani, *Weak interactions with lepton-hadron symmetry*, *Phys. Rev. D* **2** (1970) 1285.
- [54] S.L. Glashow and S. Weinberg, *Natural conservation laws for neutral currents*, *Phys. Rev. D* **15** (1977) 1958.
- [55] C. Giunti and C.W. Kim, *Fundamentals of Neutrino Physics and Astrophysics* (2007).
- [56] G.W. Anderson and L.J. Hall, *The Electroweak phase transition and baryogenesis*, *Phys. Rev. D* **45** (1992) 2685.
- [57] M. Gleiser and E.W. Kolb, *Fluctuation-driven electroweak phase transition*, *Phys. Rev. Lett.* **69** (1992) 1304.

- [58] L.-L. Chau and W.-Y. Keung, *Comments on the parametrization of the kobayashi-maskawa matrix*, *Phys. Rev. Lett.* **53** (1984) 1802.
- [59] M.E. Peskin and D.V. Schroeder, *An Introduction to quantum field theory*, Addison-Wesley, Reading, USA (1995).
- [60] H.A. Weldon, *Effective fermion masses of order  $gT$  in high-temperature gauge theories with exact chiral invariance*, *Phys. Rev. D* **26** (1982) 2789.
- [61] M.Q. Haseeb and S.S. Masood, *Two Loop Low Temperature Corrections to Electron Self Energy*, *Chin. Phys. C* **35** (2011) 608 [[1105.3054](#)].
- [62] E. Braaten and R.D. Pisarski, *Soft amplitudes in hot gauge theories: A general analysis*, *Nuclear Physics B* **337** (1990) 569.
- [63] M. Carrington, H. Defu and M. Thoma, *Equilibrium and non-equilibrium hard thermal loop resummation in the real time formalism*, *The European Physical Journal C* **7** (1999) 347–354.
- [64] E. Mottola and Z. Szép, *Systematics of high temperature perturbation theory: The two-loop electron self-energy in qed*, *Phys. Rev. D* **81** (2010) 025014.
- [65] S.-Y. Wang, *Gauge dependence of the fermion quasiparticle poles in hot gauge theories*, *Phys. Rev. D* **70** (2004) 065011 [[hep-ph/0406002](#)].
- [66] T. Kinoshita, *Mass singularities of feynman amplitudes*, *Journal of Mathematical Physics* **3** (1962) .
- [67] T.D. Lee and M. Nauenberg, *Degenerate systems and mass singularities*, *Phys. Rev.* **133** (1964) B1549.
- [68] J.F. Donoghue and B.R. Holstein, *Renormalization and radiative corrections at finite temperature*, *Phys. Rev. D* **28** (1983) 340.
- [69] J.F. Donoghue, B.R. Holstein and R. Robinett, *Quantum electrodynamics at finite temperature*, *Annals of Physics* **164** (1985) 233.
- [70] A. Johansson, G. Peressutti and B.-S. Skagerstam, *Quantum field theory at finite temperature: Renormalization and radiative corrections*, *Nuclear Physics B* **278** (1986) 324.
- [71] K. Ahmed and S. Saleem, *Finite-temperature and -density renormalization effects in qed*, *Phys. Rev. D* **35** (1987) 4020.
- [72] P. Arnold and O. Espinosa, *Effective potential and first-order phase transitions: Beyond leading order*, *Phys. Rev. D* **47** (1993) 3546.
- [73] J. Bernstein, *Spontaneous symmetry breaking, gauge theories, the higgs mechanism and all that*, *Rev. Mod. Phys.* **46** (1974) 7.
- [74] T. Morii, C.S. Lim and S.N. Mukherjee, *The physics of the standard model and beyond* (2004).